Theses and Dissertations

August 2016

Nonlocal Debye-Hückel Equations and Nonlocal Linearized Poisson-boltzmann Equations for Electrostatics of Electrolytes

Yi Jiang
University of Wisconsin-Milwaukee

Nonlocal Debye-Hückel Equations and Nonlocal Linearized Poisson-Boltzmann Equations for Electrostatics of Electrolytes

by

Yi Jiang

A Dissertation Submitted in

Partial Fulfillment of the

Requirements for the Degree of

Doctor of Philosophy

in Mathematics

at

The University of Wisconsin–Milwaukee

August 2016

ABSTRACT

Nonlocal Debye-Hückel Equations and Nonlocal Linearized Poisson-Boltzmann Equations for Electrostatics of Electrolytes

by

Yi Jiang

The University of Wisconsin-Milwaukee, 2016
Under the Supervision of Professor Dexuan Xie

Dielectric continuum models have been widely applied to the study of aqueous electrolytes since the early work done by Debye and Hückel in 1910s. Traditionally, they treat the water solvent as a simple dielectric medium with a permittivity constant without considering any correlation among water molecules. In the first part of this thesis, a nonlocal dielectric continuum model is proposed for predicting the electrostatics of electrolytes caused by any external charges. This model can be regarded as an extension of the traditional Debye-Hückel equation. For this reason, it is called the nonlocal Debye-Hückel equation. As one important application, this dissertation considers the case of an ionic solution with fixed charges from the atoms of a biomolecule. To avoid the singularities caused by the fixed atomic charges in Dirac-delta distribution, a solution decomposition scheme is constructed such that the Debye-Hückel equation is split into two equations: one with the analytical solution and the other one becoming well defined without any singularity. Hence, the study of the Debye-Hückel equation is simplified remarkably. Furthermore, a linearized nonlocal Debye-Hückel equation is proposed and thoroughly studied. Its analytic solution is found in algebraic expressions.

In the second part of this dissertation, two linearized nonlocal Poisson-Boltzmann equations (PBE) are proposed by using new linearization schemes. The third part of this dissertation reports the finite element algorithms and software packages for solving both the

nonlocal Debye-Hückel equation and the new linearized nonlocal PBE model. Numerical results validate the analytical solution of the nonlocal Debye-Hückel equation and the program packages, which are expected to be valuable in many electrolyte applications.

To

my parents

TABLE OF CONTENTS

LIST OF FIGURES

LIST OF TABLES

ACKNOWLEDGMENTS

Writing this dissertation is the final stage of the of my Ph. D. study at the University of Wisconsin-Milwaukee (UWM). At this very special moment, I would like to thank a number of people who gave their generous help to me during the past six years at UWM.

First of all, I wish to express my deepest and most sincere appreciation to my academic advisor, Professor Dexuan Xie. I has benefited very much from the association with him, because of his grateful advice and valuable criticism on my research work, as well as the research assistantship supports for more than three years. Professor Xie has been spending a great amount of time and effort in helping me since the first day I joined UWM. Without his guidance and support, it is not possible for me to complete this dissertation.

I am also greatly appreciated to Professor Istvan Lauko and Professor Gabriella Pinter, for offering a one-year opportunity working in their research group, which gave me a precise and pleasant learning experience. Meanwhile, I thank Professor Hans Volkmer for the valuable discussions on many seminars at UWM, which are very helpful in my research work. I also would like to say thanks to Professor Yi Ming Zou, Professor Chris Hruska, Professor Suzanne Boyd, etc. for their fantastic work of my graduate course lectures, and to Professor Bruce Wade and Professor Lei Wang for being my dissertation committee members.

During the six years living in Milwaukee, I have being very lucky to establish precious friendships with many great people. I would like to thank Mr. Jinyong Ying and Ms. Jiao Li who are my fellow colleagues, we helped each other in the work and shared a lot of enjoyable time together. I would like also thank Ms. Xiaoying Lin and her husband, Mr. Rongcan Huang who are always generous and help me a lot in my daily life. Although it is impossible to mention the names of my other friends, I thank them and give them my best wishes.

I was very lucky to get the opportunity to study and to pursuit my doctor degree at UWM. For this, I would like to thank Professor Yufei Yang, who was my master program advisor in the Hunan University, Changsha, Hunan, China. He is the one told me the information and encouraged me to study in the United States.

Most importantly, I wish I could let my parents know how much I thank them and love them. They are my strongest support for all these years since I was born, their love to me is the faith that drives me to beat the most difficult time and keep moving on my future

career.

At last, I would like to thank you all who spent time on reading this dissertation.

Yi Jiang

Chapter 1

Introduction

An aqueous electrolyte is a water solution containing charged chemical substance, which can induce an electric field. It is very common to see in the natural, and plays an important role in the study of many physical/chemical problems, especially with biomolecules involved. In principle, there are two different mathematical approaches to develop aqueous electrolyte models: the explicit solvent approach and the implicit solvent approach. In the explicit solvent approach, all the atoms are described explicitly. In particular, for a biomolecular system immersed in an aqueous electrolyte, each atom is represented by six unknown functions for its position and momentum. The Newton's second Law can then be used to determine the structural configuration, in the form of a large scale system of ordinary differential equations (c.f. [1, 2, 3]):

$$\mathbf{r} = (\mathbf{r}_1, .., \mathbf{r}_n) \qquad \text{with } \mathbf{r}_i \text{ being the position of atom } i,$$

where N is the total number of atoms, which is the sum of the number N_w of water molecules and the number N_p of atoms from a protein. However, since N_w can be very large, the size N of this MD system can be huge, causing challenge in calculation and memory storage during a MD implementation for a large molecular system. This limits the application of MD to a realistic biomolecular system.

To overcome this difficulty, several implicit solvent approaches have been proposed [4, 5, 6, 7, 8, 9, 10, 11]. It has been known that the electrostatic force is the dominate force for MD implementation [2, 12]. Hence, calculation on electrostatics plays a very important role in the study of structures, dynamics, interactions and functions of electrolytes [13, 14, 15, 16, 17]. In MD, it is done by using Coulomb's law for each pair among all charged atoms. This

scheme is simple but very expansive since all the atoms of this system have to be considered explicitly. On the other hand, based on the implicit solvent approach, Maxwell's equations (cf. [18]) can be used to calculate the electrostatics so that the effect of ionic solvent can be considered implicitly. Consequently, the total number of unknowns can be sharply reduced in MD implementation.

In the implicit solvent approach, a domain of water is treated as a uniform dielectric medium. When exposed to an external electrostatic field, the intra- and inter-molecular structure of water molecules will be affected, and in turn, an induced field will react to the external one. This phenomenon is known as the electric polarizations, and the induced field is called the polarization field. Traditionally, polarization effects of water molecules are assumed to be isotropic and local, in the sense that the strength of the polarization field is determined by the strength of the external electric field according to a constant factor, and point-by-point over the whole water domain.

The implicit solvent approach has attracted more and more attentions and has been used in the development of mathematical models for studying many dielectric systems, [19, 20, 21]. However, a lot of important characteristics of water structure are ignored in this simple treatment, such as their intermolecular correlations and network structures, which are usually referred to as the nonlocal solvent properties. It has been found that the polarization effects of water molecules are very complicated due to these nonlocal intermolecular interactions [22, 23, 24, 25]. To investigate them, about thirty years ago, Kornyshev and Vorotyntsev proposed and studied a nonlocal solvent model [26, 27]. Since then, a lot of efforts had been done to study and extend the nonlocal model, and to validate by many experiments that a nonlocal model could provide better predictions than the corresponding conventional local model in biophysical applications.

Another important topic in the model development for aqueous electrolytes is how to estimate the ionic charge density in a solvent domain. Due to the fact that ions are extremely small and able to move almost freely in the solvent, it is very difficult to determine the location of a specific ion, if not impossible. Hence, one usually turns to look for the concentration functions of ions through thermostatisitical theories, where the fast degree of freedoms of ions are averaged by statistical ensembles. In the context of continuum solvent approach, Boltzmann distribution has been commonly used to estimate the solvent charge density, re-

sulting in a popular dielectric continuum model, the nonlinear Poisson-Boltzmann equation (PBE) [8, 28, 29, 30, 31, 32, 33]. PBE is a second order partial differential equation (PDE) that can be regarded as a specific form of the one of the Maxwell's equations. In PBE, the ionic concentration function of each species is described as an exponential function, which is highly nonlinear in mathematics. Hence, its analytical solution may be acquired only in very few cases with symmetrical geometries. As a compromised to avoid this difficulty, traditionally, PBE was approximated by a linearized equation that an analytical solution can be found. This kind of techniques can be traced back to the work of Debye and Hückel almost a century ago [34]. Due to this reason, a model constructed by such techniques is often referred to the Debye-Hückel equation. Nowadays, computational methods become more popular in the study of PBE because of the progresses of numerical algorithms and computer hardwares [35, 36, 37, 38, 39, 40, 41, 33, 42]. So far, many fast and robust program software packages were developed and distributed in public domain, based on the finite element, finite different, finite volume and boundary element methods, such as such as APBS [43], Delphi [44, 45], PBEQ [46], PBSA [47], MIPBP [48] and SDPBS [49]. After being studied for several decades, the PBE model is still a hot spot in the fields of biochemistry, biophysics, bioengineering and mathematical biology.

In this dissertation, we studied electrostatics of aqueous electrolyte in a framework that combines the nonlocal solvent approach and the PBE approach. We proposed several new nonlocal dielectric continuum models in integral-differential equation forms, and reformulate them into systems of partial differential equations, such that their solution can be found more easily, by either an analytical or a numerical method. We also developed a finite element program package to solve the new models. This program package is expected to be valuable in the studies of aqueous electrolyte properties in real applications, such as electric double layer problems and biomolecular simulations.

The remaining part of this dissertation is organized as follows: Chapter 2 introduces some basic knowledges required in the modeling of biomolecular dielectric systems. In Chapter 3, a nonlocal Debye-Hückel equation was thoroughly studied, and its analytical solution was found. In Chapter 4, we propose two linearized nonlocal Poisson-Boltzmann equations by using new linearization schemes, and solve them numerically. In Chapter 5, we present some numerical results obtained by using our software program package which is developed based

on theoretical and algorithmic analysis in the previous chapters. At last, some conclusions are given in Chapter 6.

Chapter 2

Preliminary Knowledge

In this chapter, we introduce some fundamental knowledge that serves as the basis for studying electrostatics and nonlocal solvent effects. They include the Maxwell equations, the Poisson and Poisson-Boltzmann equations, the nonlocal dielectric theory and modeling scheme. We will also discuss the physical unit system used in this dissertation.

2.1 Basic theory for dielectric continuum modeling

Maxwell's equations have been widely used to study electromagnetic phenomena and have being a fundamental basis for classical Electromagnetics. They describe how electric and magnetic fields to be induced by charge and current, and to interact each other. These equations are named after the Scottish physicist James Clerk Maxwell who first found them in the 19th Century. In differential equation form, they can be written as the follows:

$$
\begin{cases}
\nabla \cdot \mathbf{D} = \rho & \text{(Gauss's law)}, \\
\nabla \times \mathbf{H} - \dfrac{\partial \mathbf{D}}{\partial t} = \mathbf{J} & \text{(Ampere's circuital law)}, \\
\nabla \times \mathbf{E} + \dfrac{\partial \mathbf{B}}{\partial t} = 0 & \text{(Faraday's law of induction)}, \\
\nabla \cdot \mathbf{B} = 0 & \text{(Gauss's law for magnetism)},
\end{cases}
\tag{2.1.1}
$$

where $\mathbf{E}$ is the electric field, $\mathbf{D}$ is the electric displacement field, ρ is the charge density in the space, $\mathbf{H}$ is the magnetic field, $\mathbf{B}$ is the magnetic flux density, and $\mathbf{J}$ is the current density. Here, the gradient operator ∇ is defined as

$$
\nabla \cdot = \left(\frac{\partial}{\partial x}, \frac{\partial}{\partial y}, \frac{\partial}{\partial z} \right),
\tag{2.1.2}
$$

where (x, y, z) denotes the spatial coordinates of a point in space $\mathbb{R}^3$.

In an electro-magnetic system, the displacement field $\mathbf{D}$ can be explained as the electric influence to the environment induced by explicit charges in the system (such as charged atoms). On the other hand, the overall electric effect is usually reflected by the electric field $\mathbf{E}$. It is generated by not only the explicit charges but also the implicit charges (such as induced charges on a dielectric interface due to polarizations). In vacuum, $\mathbf{D}$ and $\mathbf{E}$ satisfy a simple proportion relation:

$$\mathbf{D} = \epsilon_0 \mathbf{E}, \tag{2.1.3}$$

where ϵ_0 denotes the vacuum permittivity.

In Maxwell's equations, all electro-magnetic quantities are functions of spatial variable $\mathbf{r} = (x, y, z)$ and temporal variable t. Sometimes, in an electro-magnetic system, the electric field $\mathbf{E}$ can reach a stable status in the sense that it does not change with respect to time. In this case, $\mathbf{E}$ becomes to a vector function that only depends on the spatial variable $\mathbf{r}$, and there exists a scalar potential function Φ such that

$$\mathbf{E}(\mathbf{r}) = -\nabla\Phi(\mathbf{r}), \qquad \mathbf{r} \in \mathbb{R}^3. \tag{2.1.4}$$

This kind of electric field $\mathbf{E}$ is usually referred to as the *electrostatic field* and Φ is called the *electrostatic potential*. In an electrostatic system, there does not exist any electric current $\mathbf{J}$, or magnetic field $\mathbf{H}$, and the magnetic flux $\mathbf{B}$ is vanished. Consequently, the only nontrivial equation in (2.1.1) is the Gauss Law:

$$\nabla \cdot \mathbf{D}(\mathbf{r}) = \rho(\mathbf{r}). \tag{2.1.5}$$

Note that by (2.1.3) and (2.1.4), (2.1.5) can be equivalently written as

$$\nabla \cdot \mathbf{E}(\mathbf{r}) = \frac{1}{\epsilon_0}\rho(\mathbf{r}), \tag{2.1.6}$$

or as a Poisson equation

$$-\Delta\Phi(\mathbf{r}) = \frac{1}{\epsilon_0}\rho(\mathbf{r}), \tag{2.1.7}$$

where Δ denotes the Laplace operator that is defined by

$$\Delta = \nabla \cdot \nabla = \frac{\partial^2}{\partial x^2} + \frac{\partial^2}{\partial y^2} + \frac{\partial^2}{\partial z^2}. \tag{2.1.8}$$

Equations (2.1.3), (2.1.6) and (2.1.7) perfectly describe the relations among the charge distribution ρ, displacements field $\mathbf{D}$, electric field $\mathbf{E}$ and electrostatic potential Φ in an electrostatic system, but they are only valid in a vacuum. For a system involving a dielectric medium, the polarization effects must be considered. In principle, this effect is explained as the comprehensive reactions of the dielectric medium to the external electrostatic field. In Physics, the polarization effect can be modeled by assuming that there exists a polarization field $\mathbf{P}$ such that

$$\mathbf{D}(\mathbf{r}) = \epsilon_0 \mathbf{E}(\mathbf{r}) + \mathbf{P}(\mathbf{r}). \tag{2.1.9}$$

There are many different ways to specify the mathematical form of a polarization field, depending on different description on the dielectric property of the medium. Traditionally, one usually assumes that the polarization filed $\mathbf{P}$ responds to the electrostatic field $\mathbf{E}$ proportionally at each spatial position $\mathbf{r}$:

$$\mathbf{P}(\mathbf{r}) = \epsilon_0 \chi(\mathbf{r}) \mathbf{E}(\mathbf{r}), \tag{2.1.10}$$

where χ is the electric susceptibility function that measures the degree of polarization of a dielectric medium in response to the source electrostatic field.

By (2.1.10), we can rewrite (2.1.9) into

$$\mathbf{D}(\mathbf{r}) = \epsilon_0 (1 + \chi(\mathbf{r})) \mathbf{E}(\mathbf{r}) = \epsilon_0 \epsilon(\mathbf{r}) \mathbf{E}(\mathbf{r}), \tag{2.1.11}$$

where $\epsilon(\mathbf{r}) = 1 + \chi(\mathbf{r})$ is called the relative dielectric function of the medium. Applying (2.1.4) and (2.1.11) to (2.1.5), we get the Poisson dielectric equation:

$$-\nabla \cdot \big(\epsilon(\mathbf{r})\nabla\Phi(\mathbf{r})\big) = \frac{1}{\epsilon_0}\rho(\mathbf{r}), \qquad \mathbf{r} \in \mathbb{R}^3, \tag{2.1.12}$$

which gives the electrostatic potential Φ for the electric field $\mathbf{E}$ induced by the charge density ρ in a dielectric medium with the relative dielectric function ϵ.

(2.1.12) is the fundamental framework of the classic electrostatics. As a special case, we introduce the Poisson-Boltzmann equation in the next section.

2.2 Poisson-Boltzmann equation

The origin of the Poisson-Boltzmann equation (PBE) can be traced back to the independent works of Louis Gouy [50] and David Chapman [51], respectively. Due to this reason, it is also

often referred to as the Gouy-Chapmann theory. It was designed to predict the electrostatic potential distributions in a dielectric system in which a solid charged object is contacted with or immersed in an electrolyte. According to this theory, the ions dissolved in the solvent distribute more likely in a diffusion way because of their thermal activities. In particular, the local concentration of an ionic species is determined by the energy that is required to bring an ion of that type to the location from an infinitely far distance. The resulting formula for calculating ionic concentrations was found satisfying an exponential form and is usually referred to as the Boltzmann distribution in the literature.

Mathematically, the Poisson-Boltzmann equation can be described as a second order nonlinear partial differential equation satisfying two continuity interface conditions. Suppose the whole space $\mathbb{R}^3$ is split as

$$\mathbb{R}^3 = D_p \cup D_s \cup \Gamma, \tag{2.2.1}$$

where D_p is a bounded domain that holds a protein or other biomolecule, such as a lipid or nucleic acid, D_s is the solvent domain, filled with an ionic solution, and Γ is the interface between D_p and D_s which is usually set as a surface of the protein. Based on the implicit solvent approach, both D_p and D_s are treated as two uniform dielectric continuum mediums with dielectric constants ϵ_p and ϵ_s, respectively.

Under the settings as above, PBE can be derived from the classic Poisson dielectric model (2.1.12) when we set the dielectric function $\epsilon(\mathbf{r})$ and charge density ρ as piecewise functions in the following forms:

$$\epsilon(\mathbf{r}) = \begin{cases} \epsilon_p, & \mathbf{r} \in D_p, \\ \epsilon_s, & \mathbf{r} \in D_s, \end{cases} \tag{2.2.2}$$

and

$$\rho(\mathbf{r}) = \begin{cases} e_c \sum_{j=1}^{n_p} z_j \delta_{\mathbf{r}_j} & \text{in} \quad D_p, \\ e_c \sum_{i=1}^{n} Z_i M_i e^{-Z_i \frac{e_c \Phi(\mathbf{r})}{k_B T}} & \text{in} \quad D_s, \end{cases} \tag{2.2.3}$$

where we have assumed D_s contains n ionic spices with charge numbers Z_i for $i = 1, 2, \ldots, n$, e_c denotes the elementary charge, k_B is the Boltzmann constant, T is the temperature, M_i denotes the bulk concentration of spices i. Here, a molecular structure of the protein with n_p atoms has been given in a way that each atom is regarded as a solid ball with its atomic

9

charge concentrated at the center. z_j and $\mathbf{r}_j$ denote the charge number and position of atom j, for $j = 1, 2, \ldots, n_p$, respectively, and $\delta_{\mathbf{r}_j}$ denotes the Dirac delta distribution at $\mathbf{r}_j$.

As shown in (2.2.3), the charge densities in PBE are piecewisely defined in the solution domain D_p and the solvent domain D_s, respectively. In D_p, atomic charges of the biomolecule are treated as a group of points without volume, and with fixed locations and explicit charge quantities. In Mathematics, they are expressed as a sum of Dirac delta distributions. On the other hand, in the solvent domain D_s, the charge density function is defined through the ionic concentration functions of all species of ions

$$\rho(\mathbf{r}) = e_c \sum_{i=1}^{n} Z_i c_i(\mathbf{r}). \tag{2.2.4}$$

Further, for the ith species, its concentration function satisfies the following Boltzmann distribution

$$c_i(\mathbf{r}) = M_i e^{-Z_i \frac{e_c \Phi(\mathbf{r})}{k_B T}}. \tag{2.2.5}$$

In the classic electric theory, both Φ and $\mathbf{D}$ are assumed to be continuous along the outward normal direction of D_p. That is, on the interface Γ, we have the potential continuity condition,

$$\Phi(\mathbf{s}^-) = \Phi(\mathbf{s}^+), \qquad \mathbf{s} \in \Gamma, \tag{2.2.6}$$

and the flux continuity condition,

$$\mathbf{D}(\mathbf{s}^+) \cdot \mathbf{n}(\mathbf{s}) = \mathbf{D}(\mathbf{s}^+) \cdot \mathbf{n}(\mathbf{s}), \qquad \mathbf{s} \in \Gamma. \tag{2.2.7}$$

Here, $\mathbf{n}(\mathbf{s})$ represents the outward normal direction at $\mathbf{s}$ on Γ, and $\Phi(\mathbf{s}^+)$ denotes the limit value of Φ when it approaches to the point $\mathbf{s} \in \Gamma$ along its outward normal direction $\mathbf{n}(\mathbf{s})$ from outside. Namely, we define

$$\Phi(\mathbf{s}^\pm) = \lim_{\nu \to 0+} \Phi(\mathbf{s} \pm \nu \mathbf{n}(\mathbf{s})). \tag{2.2.8}$$

By using (2.1.4), (2.1.11) and (2.2.2), the flux continuity condition (2.2.7) can be equivalently written as

$$\epsilon_p \frac{\partial \Phi(\mathbf{s}^-)}{\partial \mathbf{n}(\mathbf{s})} = \epsilon_s \frac{\partial \Phi(\mathbf{s}^+)}{\partial \mathbf{n}(\mathbf{s})}, \tag{2.2.9}$$

where the directional derivative $\partial \Phi(\mathbf{s}^\pm)/\partial \mathbf{n}(\mathbf{s})$ is defined by

$$\frac{\partial \Phi(\mathbf{s}^\pm)}{\partial \mathbf{n}(\mathbf{s})} = \nabla \Phi(\mathbf{s}^\pm) \cdot \mathbf{n}(\mathbf{s}). \tag{2.2.10}$$

Substituting (2.2.2) and (2.2.3) into the Poisson dielectric model (2.1.12), and using the interface condition (2.2.6) and (2.2.9), we can obtain the Poisson-Boltzmann equation as the following second order nonlinear partial differential equation interface problem:

$$\begin{cases} -\epsilon_p \Delta \Phi(\mathbf{r}) = \dfrac{e_c}{\epsilon_0} \displaystyle\sum_{j=1}^{n_p} z_j \delta_{\mathbf{r}_j}, & \mathbf{r} \in D_p, \\[2mm] -\epsilon_s \Delta \Phi(\mathbf{r}) - \dfrac{e_c}{\epsilon_0} \displaystyle\sum_{i=1}^{n} Z_i M_i e^{-Z_i \frac{e_c \Phi(\mathbf{r})}{k_B T}} = 0, & \mathbf{r} \in D_s, \end{cases} \tag{2.2.11}$$

satisfying the interface conditions

$$\Phi(\mathbf{s}^-) = \Phi(\mathbf{s}^+), \quad \epsilon_p \frac{\partial \Phi(\mathbf{s}^-)}{\partial \mathbf{n}(\mathbf{s})} = \epsilon_s \frac{\Phi(\mathbf{s}^+)}{\partial \mathbf{n}(\mathbf{s})}, \qquad \mathbf{s} \in \Gamma. \tag{2.2.12}$$

Moreover, according to the fact that the electrostatic potential Φ vanishes when far away from the biomolecule, we have the following boundary condition

$$\Phi(\mathbf{r}) \to 0 \qquad \text{as} \quad |\mathbf{r}| \to \infty. \tag{2.2.13}$$

After being studied for several decades, the Poisson-Boltzmann equation is still a hot spot to study in many research areas, and it has been proved to be very successful in many applications, such as protein structure predictions [52, 53, 54, 55], free energy and pK_a calculations [56, 57, 58, 59, 60, 61, 62], ion channel problems [63, 64, 40], and rational drug design [65, 66, 67].

2.3 Nonlocal dielectric effects of water solvent

In the traditional dielectric continuum models, such as PBE, people do not consider any effect of interactions among water molecules in an aqueous electrolyte. As a result, this treatment usually induces a spatial point-to-point correspondence between the electrostatic field $\mathbf{E}$ and the displacement field $\mathbf{D}$, such as (2.1.11). For this reason, these models are called being of local.

In practice, when exposed in an external electric field, water molecules will behave more likely as electric dipole moments because of the unevenly distributed ion cloud around the hydrogen and oxygen atoms. These dipole moments interact with each other, as being attracted, repelled or twisted. This phenomenon is called the spatial nonlocal dielectric

property. It would force the water molecules in an aqueous electrolyte to form a network structure, especially in the area with a strong electric field. In a word, water molecules not only response the electrostatic field due to the external source charges, but also affect each others because of their internal induced charges. Hence, the polarization effect of an aqueous electrolyte essentially depends on the electrostatic field among the whole space, directly or indirectly.

2.4   A basic nonlocal dielectric theory

The earliest attempts to investigate the nonlocal dielectric effects via mathematical methods can be traced back to the pioneer works of Kornyshev and Vorotyntsev about forty years ago [26, 27]. In their papers, the electrostatic nonlocal polarization effects of water molecules were modeled as an integral over the whole solvent domain, and coupled into the framework of Poisson's equation.

In Mathematics, the nonlocal interaction between $\mathbf{D}$ and $\mathbf{E}$ can be discussed in a framework of operator equations. Suppose the whole space $\mathbb{R}^3$ is filled with water, the nonlocal polarization effect of water molecules can be described through the following operator equation which maps an electrostatic field function $\mathbf{E}$ to a polarization field function $\mathbf{P}$:

$$\mathbf{P} = \epsilon_0 \mathcal{X}(\mathbf{E}), \tag{2.4.1}$$

where $\mathcal{X} : \mathbf{U} \to \mathbf{V}$ is an operator, and $\mathbf{U}$ and $\mathbf{V}$ denote two appropriate vector function spaces.

(2.4.1) is a generalization of the classic local response of $\mathbf{P}$ to $\mathbf{E}$ in (2.1.10). Here, $\mathcal{X}$ plays a role as the simple proportional constant factor χ does in (2.1.10), but $\mathcal{X}$ is expected to reflect the property that the value of $\mathbf{P}$ at each position $\mathbf{r}$ will be affected by the values of $\mathbf{E}$ all over the space. Mathematically, it may be defined as an integral:

$$\mathbf{P} = \epsilon_0 \int_{\mathbb{R}^3} \chi(\mathbf{r}, \mathbf{r}')\mathbf{E}(\mathbf{r}')\mathrm{d}\mathbf{r}', \qquad \forall \mathbf{r} \in \mathbb{R}^3, \tag{2.4.2}$$

where $\chi(\mathbf{r}, \mathbf{r}')$ is called the susceptibility function.

In Physics, $\chi(\mathbf{r}, \mathbf{r}')$ describes the electrostatic correspondence between two water molecules locating at position $\mathbf{r}$ and $\mathbf{r}'$, respectively. Ideally, the value of $\chi(\mathbf{r}, \mathbf{r}')$ is determined by the status of these two water molecules, including their distance, relative angles and internal

structures. However, it would be extremely difficult to investigate χ if all these factor are taken into account. To simplify the discussion, all water molecules are usually assumed to be isotropical and distributed uniformly over the solvent domain, such that the value of function χ depends only on the difference $\mathbf{r} - \mathbf{r}'$:

$$\chi(\mathbf{r}, \mathbf{r}') = \chi(\mathbf{r} - \mathbf{r}'). \tag{2.4.3}$$

Accordingly, (2.4.2) becomes a convolution

$$\mathbf{P} = \epsilon_0 \int_{\mathbb{R}^3} \chi(\mathbf{r} - \mathbf{r}')\mathbf{E}(\mathbf{r}')\mathrm{d}\mathbf{r}', \qquad \forall \mathbf{r} \in \mathbb{R}^3, \tag{2.4.4}$$

with χ denoting the convolution kernel function.

In principle, there are many different kinds of nonlocal polarizations, and one specific type determines one specific form of the kernel function χ. Among them, there is a well-known and thoroughly investigated model, named the Fourier-Lorenztian model, which can be defined via a Lorentzian function in the frequency space under the Fourier transform (cf. [68, 69, 70]):

$$\hat{\chi}(k) = \chi_\infty + \frac{\chi_s - \chi_\infty}{1 + \lambda^2 k^2}, \tag{2.4.5}$$

where χ_s and χ_∞ are the susceptibilities of water molecules for static and optical cases, respectively, λ is usually explained as the nonlocal correlation length which indicates the range that the intermolecular interactions between each pair of water molecules is significant, and k denotes the norm of the frequency space variable $\mathbf{k}$. By inverse the Fourier transform, the expression of χ in the spatial space can be found as:

$$\chi(r) = \chi_\infty \delta_r + (\chi_s - \chi_\infty)\frac{e^{-r/\lambda}}{4\pi\lambda^2 r}, \tag{2.4.6}$$

where r denotes the norm of spatial variable $\mathbf{r}$, and δ is the Dirac Delta distribution at r.

Based on all above arguments, we now can induce a specific nonlocal relation between the displacement field $\mathbf{D}$ and the electric field $\mathbf{E}$ as

$$\begin{aligned}
\mathbf{D}(\mathbf{r}) =& \epsilon_0 \mathbf{E}(\mathbf{r}) + \mathbf{P}(\mathbf{r}) \\
=& \epsilon_0 \mathbf{E}(\mathbf{r}) + \epsilon_0 \mathcal{X}(\mathbf{E})(\mathbf{r}) \\
=& \epsilon_0 \mathbf{E}(\mathbf{r}) + \epsilon_0 \left(\chi_\infty \mathbf{E}(\mathbf{r}) + (\chi_s - \chi_\infty) \int_{\mathbb{R}^3} \frac{e^{-|\mathbf{r}-\mathbf{r}'|/\lambda}}{4\pi\lambda^2 |\mathbf{r} - \mathbf{r}'|} \mathbf{E}(\mathbf{r}')\mathrm{d}\mathbf{r}' \right) \\
=& \epsilon_0 \left(\epsilon_\infty \mathbf{E}(\mathbf{r}) + (\epsilon_s - \epsilon_\infty) \int_{\mathbb{R}^3} \frac{e^{-|\mathbf{r}-\mathbf{r}'|/\lambda}}{4\pi\lambda^2 |\mathbf{r} - \mathbf{r}'|} \mathbf{E}(\mathbf{r}')\mathrm{d}\mathbf{r}' \right), \qquad \mathbf{r} \in \mathbb{R}^3,
\end{aligned} \tag{2.4.7}$$

13

where we have defined

$$\epsilon_\infty = 1 + \chi_\infty \tag{2.4.8}$$

as a new dielectric parameter of water medium that corresponds to the limit case when water molecules vibrate in high frequency.

For clarification, we conclude our results in the following proposition:

Proposition 2.4.1. *Under the effects of nonlocal solvent polarizations, the displacement field* $\mathbf{D}$ *interacts with the electrostatic field* $\mathbf{E}$ *according to the operator equation:*

$$\mathbf{D} = \epsilon_0 \mathcal{E}(\mathbf{E}), \tag{2.4.9}$$

where $\mathcal{E} : \mathbf{U} \to \mathbf{V}$ *is an operator for two appropriate vector function spaces* $\mathbf{U}$ *and* $\mathbf{V}$*, which reflects the nonlocal effects.*

As a special case, operator $\mathcal{E}$ *can be defined by the Fourier-Lorentzian model, such that*

$$\mathbf{D}(\mathbf{r}) = \epsilon_0 \left(\epsilon_\infty \mathbf{E}(\mathbf{r}) + (\epsilon_s - \epsilon_\infty) \int_{\mathbb{R}^3} \frac{e^{-|\mathbf{r}-\mathbf{r}'|/\lambda}}{4\pi\lambda^2|\mathbf{r}-\mathbf{r}'|} \mathbf{E}(\mathbf{r}')\mathrm{d}\mathbf{r}' \right), \qquad \mathbf{r} \in \mathbb{R}^3. \tag{2.4.10}$$

Usually, people are more interested in the electrostatic potential Φ. Thus, substituting (2.4.10) into the Gauss law (2.1.5), and use the fact $\mathbf{E} = -\nabla\Phi$, we get the following nonlocal dielectric Poisson equation:

$$-\nabla \cdot \left(\epsilon_\infty \nabla \Phi(\mathbf{r}) + (\epsilon_s - \epsilon_\infty) \int_{\mathbb{R}^3} \frac{e^{-|\mathbf{r}-\mathbf{r}'|/\lambda}}{4\pi\lambda^2|\mathbf{r}-\mathbf{r}'|} \nabla \Phi(\mathbf{r}')\mathrm{d}\mathbf{r}' \right) = \frac{1}{\epsilon_0}\rho. \tag{2.4.11}$$

2.5 Solution decomposition techniques

Solution decomposition techniques are commonly used in searching for the solution of the Poisson equation and its variants. To show the basic principle, we define a Poisson-like equation written in the operator form as follows

$$L(\Phi) = \rho \qquad \text{in} \quad \Omega, \tag{2.5.1}$$

subject to the boundary condition

$$B(\Phi) = g \qquad \text{on} \quad \partial\Omega, \tag{2.5.2}$$

where ρ is the charge density in the domain Ω, L and B denote two operators, and g is a boundary value function. We would like to decompose the solution Φ into n components:

$$\Phi = \Phi_1 + \Phi_2 + \cdots + \Phi_n. \tag{2.5.3}$$

Accordingly, $L(\Phi)$ and ρ are split as

$$L(\Phi) = L_1(\Phi_1, \Phi_2, \ldots, \Phi_n) + L_2(\Phi_1, \Phi_2, \ldots, \Phi_n) + L_n(\Phi_1, \Phi_2, \ldots, \Phi_n), \tag{2.5.4}$$

and

$$\rho = \rho_1 + \rho_2 + \cdots + \rho_n, \tag{2.5.5}$$

such that these components satisfy the following system of equations:

$$\begin{cases} L_1(\Phi_1, \Phi_2, \ldots, \Phi_n) = \rho_1, \\ L_2(\Phi_1, \Phi_2, \ldots, \Phi_n) = \rho_2, \\ \qquad \ldots \\ L_n(\Phi_1, \Phi_2, \ldots, \Phi_n) = \rho_n. \end{cases} \tag{2.5.6}$$

For each of the above equations, its boundary or interface conditions shall be constructed from the original condition $B(\Phi) = g$. We expect that a solution of the above system can be found more easily in comparison to the case of solving the original equation.

Several solution decomposition techniques have been proposed in case of Poisson-Boltzmann equation. By them, the decomposition of a PBE solution can be restricted to a subdomain (D_p or D_s) or applied to the whole space. Usually, the solution of PBE is split into two or three components, one of which is a function with known algebraic formula that catches all singularities induced by Dirac delta distributions. As an example, in the following, we present a decomposition scheme of PBE that was proposed in [33] (theorem 3.1). Other different solution decomposition technique used for solving PBE can be found in [36, 71, 72, 73].

Proposition 2.5.1. *The solution Φ of (2.2.11) can be decomposed into three parts:*

$$\Phi = G + \Psi + \Phi, \tag{2.5.7}$$

where G is defined as

$$G = \frac{e_c^2}{4\pi\epsilon_0\epsilon_s k_B T} \sum_{j=1}^{n_p} \frac{z_j}{|\mathbf{r} - \mathbf{r}_j|}, \tag{2.5.8}$$

15

Ψ *satisfies the following linear interface problem*

$$\begin{cases} \Delta\Psi(\mathbf{r}) = 0, & \mathbf{r} \in D_p \cup D_s, \\ \epsilon_p\Psi(\mathbf{s}^-) = \epsilon_s\Psi(\mathbf{s}^+), & \mathbf{s} \in \Gamma, \\ \epsilon_p\dfrac{\partial\Psi(\mathbf{s}^-)}{\partial\mathbf{n}(\mathbf{s})} = \epsilon_s\dfrac{\partial\Psi(\mathbf{s}^+)}{\partial\mathbf{n}(\mathbf{s})} + (\epsilon_s - \epsilon_p)\dfrac{\partial G(\mathbf{s})}{\partial\mathbf{n}(\mathbf{s})}, & \mathbf{s} \in \Gamma, \\ \Psi(\mathbf{r}) \to 0, & as \quad |\mathbf{r}| \to 0, \end{cases} \qquad (2.5.9)$$

and $\tilde{\Phi}$ *satisfies the following nonlinear interface problem*

$$\begin{cases} -\epsilon_p\Delta\tilde{\Phi}(\mathbf{r}) = 0, & \mathbf{r} \in D_p, \\ -\epsilon_s\Delta\tilde{\Phi}(\mathbf{r}) - \dfrac{e_c^2}{\epsilon_0 k_B T}\displaystyle\sum_{i=1}^{n} Z_i M_i e^{-Z_i(G(\mathbf{r})+\Psi(\mathbf{r})+\tilde{\Phi}(\mathbf{r}))} = 0, & \mathbf{r} \in D_s, \\ \epsilon_p\tilde{\Phi}(\mathbf{s}^-) = \epsilon_s\tilde{\Phi}(\mathbf{s}^+), \quad \epsilon_p\dfrac{\partial\tilde{\Phi}(\mathbf{s}^-)}{\partial\mathbf{n}(\mathbf{s})} = \epsilon_s\dfrac{\partial\tilde{\Phi}(\mathbf{s}^+)}{\partial\mathbf{n}(\mathbf{s})}, & \mathbf{s} \in \Gamma, \\ \tilde{\Phi}(\mathbf{r}) \to 0, & as \quad |\mathbf{r}| \to 0. \end{cases} \qquad (2.5.10)$$

Comparing to the original PBE, we can obtain the following advantages by using the decomposition formula of (2.5.7):

- All the singularities are taken out from the PBE solution to form function G whose analytical expression is known.

- The jump flux interface condition occurs only in the linear problem for solving Ψ, such that the nonlinear problem for solving $\tilde{\Phi}$ has a simpler continuous flux interface condition.

- The three components of Φ have a clear physical explanation:

  1. G is the potential induced by the explicit fixed charges from the protein.

  2. Ψ is the electrostatic potential induced by the implicit surface charge due to the dielectric jump across the interface Γ.

  3. $\tilde{\Phi}$ is the electrostatic potential induced by the charges of ions in the solvent.

- The solution decomposition leads to an efficient algorithm for finding the solution Φ as follows:

  1. Calculate G by (2.5.8).

16

2. Solve Ψ by (2.5.9).

3. Solve $\tilde{\Phi}$ by (2.5.10).

4. Obtain $\Phi = G + \Psi + \tilde{\Phi}$.

2.6 Physical parameters and units

There exist different physical unit systems to describe various models. In this thesis, we only consider the equations under the SI unit system [74], in which the electrostatic potential, Φ, and its components are measured in Volts. For clarity, we list all the parameters of PBE in Table 2.1, along with their physical meanings and units.

Table 2.1: Magnitudes & Units of PBE parameters in SI unit system

	Concepts	Units(abbr.)	Magnitudes
ϵ_0	Permittivity of vacuum	Farad/Meter(F/m)	$8.854187817 \times 10^{-12}$
e_c	Elementary charge	Coulomb(C)	$1.602176565 \times 10^{-19}$
T	Absolute temperature	Kelvin(K)	298.15
k_B	Boltzmann constant	Joule/Kelvin(J/K)	$1.380648813 \times 10^{-23}$

Besides, the related dimensionless physical constants are listed shown in Table 2.2.

Table 2.2: Physical Constants

	Concepts	Magnitudes
ϵ_p	Dielectric constant of protein in D_p	2.0
ϵ_s	Dielectric constant of water in D_s	78.5
$\mathcal{N}_a$	Alvogadro's constant	6.0220450×10^{23}

To simplify calculation, we can transfer PBE to a dimensionless form. The basic principle is to multiply the electrostatic potential, Φ by the constant $e_c/k_B T$, such that the product $e_c\Phi/k_B T$ takes no dimension. Same manipulations can be applied to the components of Φ, such as G, Ψ and $\tilde{\Phi}$ induced from the decomposition scheme as shown in Proposition 2.5.1. If we keep the same notation, i.e.,

$$\frac{e_c}{k_B T}\Phi \to \Phi, \qquad \frac{e_c}{k_B T}\Psi \to \Psi, \qquad \frac{e_c}{k_B T}G \to G, \qquad (2.6.1)$$

then, the Poisson equation (2.6.2) is written in the dimensionless form:

$$- \nabla \cdot \big(\epsilon(\mathbf{r})\nabla\Phi(\mathbf{r})\big) = \frac{e_c}{\epsilon_0 k_B T}\rho(\mathbf{r}), \qquad \mathbf{r} \in \mathbb{R}^3, \tag{2.6.2}$$

and the Poisson-Boltzmann equation (2.2.11) has the dimensionless form:

$$\begin{cases} -\epsilon_p \Delta\Phi(\mathbf{r}) = \dfrac{e_c^2}{\epsilon_0 k_B T}\displaystyle\sum_{j=1}^{n_p} z_j \delta_{\mathbf{r}_j}, & \mathbf{r} \in D_p, \\[2mm] -\epsilon_s \Delta\Phi(\mathbf{r}) + \dfrac{e_c^2}{\epsilon_0 k_B T}\displaystyle\sum_{i=1}^{n} Z_i M_i e^{-Z_i \Phi(\mathbf{r})} = 0, & \mathbf{r} \in D_s. \end{cases} \tag{2.6.3}$$

Note that the new interface conditions have the same forms as the ones given in (2.2.12).

Usually, this dimensionless setting can simplify the study and solution of the Poisson equation and PBE. In the rest of the paper, we will restrict our discussions to their dimensionless forms.

Chapter 3

Nonlocal Debye-Hückel Equations

The classic Debye-Hückel equation is a continuum model for investigating electrostatic properties of ionic solution. It was first proposed by Peter Debye and Erich Hückel for calculating the activity coefficient of ionic solutions [34]. In their thesis, they pointed out that dissolved ions in a solution do not distribute ideally when exposed to an external electrostatic field, due to the electric interactions among them. Mathematically, the Debye-Hückel equation is usually described as a second order linear partial differential equation. As a quick review, we will first follow the Poisson-Boltzmann theory to derive a nonlinear Debye-Hückel equation. We then will couple it with the nonlocal dielectric properties to propose and investigate several nonlocal Debye-Hückel equations.

3.1 A nonlinear Debye-Hückel equation

Let the whole space $\mathbb{R}^3$ be filled with an ionic solution containing n ionic species, and be treated as one continuum medium with the dielectric constant ϵ_s. Two charge density functions, ρ_f and ρ_m, are given to denote the fixed charges and ionic mobile charges, respectively, such that the total charge density function ρ is given by

$$\rho = \rho_f + \rho_m. \tag{3.1.1}$$

Hence, by (2.1.12), the electrostatic potential, Φ, can be determined by Poisson's equation in the dimensionless form:

$$-\epsilon_s \Delta \Phi(\mathbf{r}) = \frac{e_c}{\epsilon_0 k_B T}(\rho_f(\mathbf{r}) + \rho_m(\mathbf{r})), \qquad \mathbf{r} \in \mathbb{R}^3. \tag{3.1.2}$$

Usually, it is easy to get ρ_f in many real applications, but how to estimate ρ_m is challenging, which remains a research topic by itself. In this section, we assume that there exist ionic concentration functions, c_i, for $i = 1, 2, \ldots, n$, such that

$$\rho_m(\mathbf{r}) = \frac{e_c^2}{\epsilon_0 k_B T} \sum_{i=1}^{n} Z_i c_i(\mathbf{r}), \tag{3.1.3}$$

where e_c is the elementary charge, and Z_i is the charge number of the i-th ionic species.

To simplify calculation, we apply a solution decomposition technique to (3.1.2) to split Φ as

$$\Phi = G + \Psi, \tag{3.1.4}$$

where G and Ψ are the solutions of the following two equations, respectively:

$$\begin{cases} -\epsilon_s \Delta G(\mathbf{r}) = \dfrac{e_c}{\epsilon_0 k_B T} \rho_f(\mathbf{r}), & \mathbf{r} \in \mathbb{R}^3, \\ \qquad G(\mathbf{r}) \to 0 & \text{as} \quad |\mathbf{r}| \to \infty, \end{cases} \tag{3.1.5}$$

and

$$\begin{cases} -\epsilon_s \Delta \Psi(\mathbf{r}) = \dfrac{e_c^2}{\epsilon_0 k_B T} \sum_{i=1}^{n} Z_i c_i(\mathbf{r}), & \mathbf{r} \in \mathbb{R}^3, \\ \qquad \Psi(\mathbf{r}) \to 0 & \text{as} \quad |\mathbf{r}| \to \infty. \end{cases} \tag{3.1.6}$$

Since G is determined by ρ_f only, it is independent of c. Hence, we only need to consider the equation (3.1.6) to search for the optimal electrostatic potential Φ.

For simplicity, we restrict our discussion on a bounded domain Ω satisfying the following conditions:

1. Ω is large enough such that it contains all the fixed charges.

2. Φ satisfies a homogeneous Dirichlet boundary condition, $\Phi|_{\partial\Omega} = 0$, where $\partial\Omega$ denotes the boundary of Ω.

An inhomogeneous boundary condition can be discussed similarly as what was done in [75].

Let $c = (c_1, c_2, \ldots, c_n)$. According to the Poisson-Boltzmann theory, we determine an optimal c as a solution of the following partial differential equation constrained minimization problem:

$$\min_{c \in V, \Psi \in U} F(c, \Psi) \tag{3.1.7}$$

20

subject to Poisson's equation

$$
\begin{cases}
-\epsilon_s \Delta \Psi(\mathbf{r}) = \dfrac{e_c^2}{\epsilon_0 k_B T} \displaystyle\sum_{i=1}^{n} Z_i c_i(\mathbf{r}), & \mathbf{r} \in \Omega, \\[2mm]
\Psi(\mathbf{s}) = -G(\mathbf{s}), & \mathbf{s} \in \partial\Omega,
\end{cases}
\tag{3.1.8}
$$

where V and U denote two appropriate function spaces, F is an energy functional defined by

$$
F(c, \Psi) = F_{es}(c, \Psi) + F_{id}(c) + F_G(c).
\tag{3.1.9}
$$

Here, the electrostatic energy term F_{es} is defined by

$$
F_{es}(c, \Psi) = \frac{k_B T}{2 e_c} \int_{\Omega} \rho_f(\mathbf{r}) \Psi(\mathbf{r}) \mathrm{d}\mathbf{r} + \frac{k_B T}{2} \sum_{i=1}^{n} Z_i \int_{\Omega} c_i(\mathbf{r}) \big[G(\mathbf{r}) + \Psi(\mathbf{r}) \big] \mathrm{d}\mathbf{r},
\tag{3.1.10}
$$

the idea gas energy term F_{id} is defined by

$$
F_{id}(c) = k_B T \sum_{i=1}^{n} \int_{\Omega} c_i(\mathbf{r}) \big[\ln(c_i(\mathbf{r})\Lambda_i^3) - 1 \big] \mathrm{d}\mathbf{r},
\tag{3.1.11}
$$

and the Gibbs free energy term F_G is defined by

$$
F_G(c) = -\sum_{i=1}^{n} \mu_i \int_{\Omega} c_i(\mathbf{r}) \mathrm{d}\mathbf{r},
\tag{3.1.12}
$$

where Λ_i and μ_i are the de Broglie wavelength and the chemistry potential of the i-th ionic species, respectively.

Usually, the fixed charges are assumed to be a set of point charges from a structure of a protein molecule. In this case, ρ_f is defined by

$$
\rho_f = e_c \sum_{j=1}^{n_p} z_j \delta_{\mathbf{r}_j},
\tag{3.1.13}
$$

where z_j and $\mathbf{r}_j$ denote the charge number and position of atom j, and n_p is the number of all atoms of the protein. For the above ρ_f, the analytic solution of (3.1.5) can be found in the formula:

$$
G(\mathbf{r}) = \frac{e_c^2}{4\pi \epsilon_0 \epsilon_s k_B T} \sum_{j=1}^{n_p} \frac{z_j}{|\mathbf{r} - \mathbf{r}_j|}.
\tag{3.1.14}
$$

21

Next we consider the solution existence and uniqueness of (3.1.8). Let $C(\Omega)$ and $C^2(\Omega)$ denote the function spaces for continuous and second-order continuously differentiable functions defined on Ω, respectively. We assume $c_i \in C(\Omega)$ for $i = 1, 2, \ldots, n$. Since the linear operator $\Delta : C^2(\Omega) \rightarrow C(\Omega)$ is positive, continuous, and self-adjoint, its inverse $\Delta^{-1} : C(\Omega) \rightarrow C^2(\Omega)$ exists. Thus, Ψ can be expressed in the operator form:

$$\Psi = -\frac{e_c^2}{\epsilon_0 \epsilon_s k_B T} \sum_{i=1}^{n} Z_i \Delta^{-1}(c_i), \tag{3.1.15}$$

Because of (3.1.15), we can regard Ψ as a function of ionic concentrations functions c, denoted as $\Psi = \Psi(c)$. Hence, by (3.1.9), we can define a function of c, $f(c)$, as

$$f(c) = F(c, \Psi(c)). \tag{3.1.16}$$

Let $f'(c)$ and $f''(c)$ denote the first and second Fréchet differentials of f at c, which are respectively defined as

$$f'(c)v = \sum_{i=1}^{n} \frac{\partial f(c)}{\partial c_i} v_i \qquad \text{and} \qquad f''(c)(v, w) = \sum_{i,j=1}^{n} \frac{\partial^2 f(c)}{\partial c_j \partial c_i} v_i w_j,$$

where $v = (v_1, v_2, \ldots, v_n)$ and $w = (w_1, w_2, \ldots, w_n)$ with $v_i, w_j \in L^2(\Omega)$ for $i, j = 1, 2, \ldots, n$, and $\frac{\partial f(c)}{\partial c_i}$ and $\frac{\partial^2 f(c)}{\partial c_j \partial c_i}$ denote the first and second order partial derivatives of f, respectively.

Following what was done in [42], we can show that the energy functional f is strictly convex so that the minimization problem (3.1.7) has a unique local minimizer, which is also the global minimizer. For clarity, we collect some important results as follows:

1. The first and second Fréchet derivatives f' and f'' can be found in the forms:

$$f'(c)v = \sum_{i=1}^{n} \int_{\Omega} [Z_i k_B T \Phi(\mathbf{r}) + k_B T \ln(c_i(\mathbf{r}) \Lambda_i^3) - \mu_i] v_i(\mathbf{r}) d\mathbf{r},$$

and

$$f''(c)(v, w) = k_B T \sum_{i,j=1}^{n} Z_i Z_j e_c^2 \int_{\Omega} L^{-1} v_i(\mathbf{r}) w_j(\mathbf{r}) d\mathbf{r} + k_B T \sum_{i=1}^{n} \int_{\Omega} \frac{1}{c_i} v_i w_i d\mathbf{r},$$

for any $v, w \in V$. Here, the operator $L : U \rightarrow L^2(\Omega)$ is defined as follows:

$$\langle Lu, v \rangle_{L^2(\Omega)} = \epsilon_s \int_{\Omega} \nabla u \cdot \nabla v d\mathbf{r}, \qquad \forall u, v \in U. \tag{3.1.17}$$

22

2. The second derivative $f''(c)$ is positive definite. Thus, f is strictly convex and has a unique local minimal point $c^* = (c_1^*, c_2^*, \ldots, c_n^*)$, which is also the global minimal point.

3. The minimizer c^* can be found by the following first order optimization condition

$$f'(c^*) = 0. \tag{3.1.18}$$

4. By solving (3.1.18), each c_i^* can be represented in the Boltzmann distribution:

$$c_i^*(\mathbf{r}) = M_i e^{-Z_i \Phi^*(\mathbf{r})}, \qquad i = 1, 2, \ldots, n, \tag{3.1.19}$$

where the constant $M_i = \Lambda_i^{-3} e^{\mu_i / k_B T}$ that is often explained as the average concentration of the ith species of ions. Correspondingly, the mobile charge density function ρ_m has the following form

$$\rho_m(\mathbf{r}) = e_c \sum_{i=1}^n Z_i c_i^*(\mathbf{r}) = e_c \sum_{i=1}^n Z_i M_i e^{-Z_i \Phi^*(\mathbf{r})}. \tag{3.1.20}$$

5. By (3.1.4), the optimal electrostatic potential is obtained by

$$\Phi^* = \Psi(c^*) + G. \tag{3.1.21}$$

Substituting the Boltzmann distribution (3.1.19) into (3.1.6), we can get a nonlinear Debye-Hückel equation as follows:

$$\begin{cases} -\epsilon_s \Delta \Phi(\mathbf{r}) - \dfrac{e_c^2}{\epsilon_0 k_B T} \sum_{i=1}^n Z_i M_i e^{-Z_i \Phi(\mathbf{r})} = \dfrac{e_c^2}{\epsilon_0 k_B T} \sum_{j=1}^{n_p} z_j \delta_{\mathbf{r}_j}, & \mathbf{r} \in \Omega, \\ \Phi(\mathbf{s}) = 0, & \mathbf{s} \in \partial\Omega. \end{cases} \tag{3.1.22}$$

We conclude the above arguments in the following theorem:

Theorem 3.1.1. *The minimization problem* (3.1.7) *is equivalent to the nonlinear Debye-Hückel equation* (3.1.22), *with the minimizer* c_i *being given in* (3.1.19).

As a typical case, for a symmetric 1:1 monovalent ionic solution, such as NaCl aqueous solution, we have $n = 2$, $Z_1 = 1$, $Z_2 = -1$, and $M_1 = M_2 = M$, where M denotes a given bulk

concentration of the salt dissolved in the solution. In this case, the nonlinear Debye-Hückel equation becomes

$$
\begin{cases}
-\epsilon_s \Delta \Phi(\mathbf{r}) + \dfrac{2Me_c^2}{\epsilon_0 k_B T} \sinh\left(\Phi(\mathbf{r})\right) = \dfrac{e_c^2}{\epsilon_0 k_B T} \sum_{j=1}^{n_p} z_j \delta_{\mathbf{r}_j}, & \mathbf{r} \in \mathbb{R}^3, \\
\Phi(\mathbf{s}) = 0, & \mathbf{s} \in \partial\Omega.
\end{cases}
\tag{3.1.23}
$$

In the case that the potential magnitude $|\Phi|$ is sufficiently close to zero, the hyperbolic term in (3.1.23) may be approximated by:

$$
\sinh\left(\Phi(\mathbf{r})\right) \approx \Phi(\mathbf{r}).
\tag{3.1.24}
$$

Consequently, (3.1.23) is simplified to the traditional Debye-Hückel equation:

$$
\begin{cases}
-\epsilon_s \Delta \Phi(\mathbf{r}) + \dfrac{2Me_c^2}{\epsilon_0 k_B T} \Phi(\mathbf{r}) = \dfrac{e_c^2}{\epsilon_0 k_B T} \sum_{j=1}^{n_p} z_j \delta_{\mathbf{r}_j}, & \mathbf{r} \in \mathbb{R}^3, \\
\Phi(\mathbf{s}) = 0, & \mathbf{s} \in \partial\Omega.
\end{cases}
\tag{3.1.25}
$$

It is well known that the solution of the above equation has the following form:

$$
\Phi(\mathbf{r}) = \frac{e_c^2}{4\pi\epsilon_0 \epsilon_s k_B T} \sum_{j=1}^{n_p} \frac{e^{-\kappa|\mathbf{r}-\mathbf{r}_j|}}{|\mathbf{r}-\mathbf{r}_j|}, \qquad \forall \mathbf{r} \in \mathbb{R}^3, \quad \mathbf{r} \neq \mathbf{r}_j,
\tag{3.1.26}
$$

where the constant κ is defined by

$$
\kappa = \sqrt{\frac{2Me_c^2}{\epsilon_0 \epsilon_s k_B T}}
\tag{3.1.27}
$$

which is called the inverse Debye length.

3.2   A nonlocal Debye-Hückel equation

In this section, we derive a nonlocal Debye-Hückel equation from the basic nonlocal dielectric Poisson equation (2.4.11).

Clearly, the dimensionless form of (2.4.11) can be obtained as follows:

$$
\begin{cases}
-\epsilon_\infty \Delta \Phi(\mathbf{r}) + (\epsilon_s - \epsilon_\infty)\nabla \cdot \displaystyle\int_{\mathbb{R}^3} Q_\lambda(\mathbf{r}-\mathbf{r}')\nabla\Phi(\mathbf{r}')d\mathbf{r}' = \dfrac{e_c}{\epsilon_0 k_B T}\rho(\mathbf{r}), & \mathbf{r} \in \mathbb{R}^3, \\
\Phi(\mathbf{r}) \to 0 & \text{as } |\mathbf{r}| \to \infty,
\end{cases}
\tag{3.2.1}
$$

24

where Q_λ is defined as a Poisson kernel:

$$Q_\lambda(\mathbf{r}) = \frac{1}{4\pi\lambda^2|\mathbf{r}|}e^{-|\mathbf{r}|/\lambda}, \qquad \mathbf{r} \neq 0. \qquad (3.2.2)$$

Similar to the case of the traditional Debye-Hückel equation, we defined the charge density ρ by

$$\begin{aligned}\rho(\mathbf{r}) &= \rho_f(\mathbf{r}) + \rho_m(\mathbf{r}) \\ &= e_c \sum_{j=1}^{n_p} z_j \delta_{\mathbf{r}_j} + e_c \sum_{i=1}^{n} Z_i M_i e^{-Z_i\Phi(\mathbf{r})}.\end{aligned} \qquad (3.2.3)$$

Applying the above ρ into (3.2.1), we get the nonlinear nonlocal Debye-Hückel equation:

$$\begin{cases} -\epsilon_\infty\Delta\Phi(\mathbf{r}) + (\epsilon_s - \epsilon_\infty)\nabla \cdot \displaystyle\int_{\mathbb{R}^3} Q_\lambda(\mathbf{r} - \mathbf{r}')\nabla\Phi(\mathbf{r}')d\mathbf{r}' \\ \qquad - \dfrac{e_c^2}{\epsilon_0 k_B T}\displaystyle\sum_{i=1}^{n} Z_i M_i e^{-Z_i\Phi(\mathbf{r})} = \dfrac{e_c^2}{\epsilon_0 k_b T}\displaystyle\sum_{j=1}^{n_p} z_j\delta_{\mathbf{r}_j}, \\ \qquad\qquad \Phi(\mathbf{r}) \to 0 \qquad \text{as} \quad |\mathbf{r}| \to \infty. \end{cases} \qquad (3.2.4)$$

For the typical 1:1 ionic solution, the above equation can be simplified as

$$\begin{cases} -\epsilon_\infty\Delta\Phi(\mathbf{r}) + (\epsilon_s - \epsilon_\infty)\nabla \cdot \displaystyle\int_{\mathbb{R}^3} Q_\lambda(\mathbf{r} - \mathbf{r}')\nabla\Phi(\mathbf{r}')d\mathbf{r}' \\ \qquad + \dfrac{2Me_c^2}{\epsilon_0 k_B T}\sinh(\Phi(\mathbf{r})) = \dfrac{e_c^2}{\epsilon_0 k_B T}\displaystyle\sum_{j=1}^{n_p} z_j\delta_{\mathbf{r}_j}, \qquad \mathbf{r} \in \mathbb{R}^3, \\ \qquad\qquad \Phi(\mathbf{r}) \to 0 \qquad\qquad\qquad\qquad \text{as} \quad |\mathbf{r}| \to \infty. \end{cases} \qquad (3.2.5)$$

In the case that $|\Phi(\mathbf{r})|$ is small enough, the above nonlinear equation can be linearized into

$$\begin{cases} -\epsilon_\infty\Delta\Phi(\mathbf{r}) + (\epsilon_s - \epsilon_\infty)\nabla \cdot \displaystyle\int_{\mathbb{R}^3} Q_\lambda(\mathbf{r} - \mathbf{r}')\nabla\Phi(\mathbf{r}')d\mathbf{r}' \\ \qquad + \dfrac{2Me_c^2}{\epsilon_0 k_B T}\Phi(\mathbf{r}) = \dfrac{e_c^2}{\epsilon_0 k_B T}\displaystyle\sum_{j=1}^{n_p} z_j\delta_{\mathbf{r}_j}, \qquad \mathbf{r} \in \mathbb{R}^3, \\ \qquad\qquad \Phi(\mathbf{r}) \to 0 \qquad\qquad\qquad\qquad \text{as} \quad |\mathbf{r}| \to \infty. \end{cases} \qquad (3.2.6)$$

Clearly, when ϵ_∞ approaches to ϵ_s, (3.2.6) reduces to the traditional Debye-Hückel equation (3.1.25). Due to this reason, we will call (3.2.6) the nonlocal Debye-Hückel equation for clarity.

3.3　Derivation of analytical solutions

In this section, we present the analytic solution of the nonlocal Debye-Hückel equation (3.2.6). By the superposition principal, we only need to calculate the fundamental solution of the following problem:

$$\begin{cases} -\epsilon_\infty \Delta \Phi(\mathbf{r}) + (\epsilon_s - \epsilon_\infty)\nabla \cdot \int_{\mathbb{R}^3} Q_\lambda(\mathbf{r} - \mathbf{r}')\nabla\Phi(\mathbf{r}')\mathrm{d}\mathbf{r}' + \bar{\kappa}^2\Phi(\mathbf{r}) = \delta, & \mathbf{r} \in \mathbb{R}^3, \\ \Phi(\mathbf{r}) \to 0, & \text{as } |\mathbf{r}| \to \infty, \end{cases}$$

(3.3.1)

where $\bar{\kappa}$ is defined by

$$\bar{\kappa} = \sqrt{\epsilon_s}\kappa = \sqrt{\frac{2Me_c^2}{\epsilon_0 k_B T}}.$$

(3.3.2)

First, we notice that Q_λ is the fundamental solution of the following partial differential equation:

$$-\lambda^2 \Delta Q_\lambda + Q_\lambda = \delta.$$

(3.3.3)

Taking convolutions with Φ on both sides, and using the multiplication property of convolution, we get

$$-\lambda^2 \Delta (Q_\lambda * \Phi) + Q_\lambda * \Phi = \Phi.$$

(3.3.4)

Regarding $Q_\lambda * \Phi$ as an auxiliary function, the above can be written as

$$-\lambda^2 \Delta u + u - \Phi = 0,$$

(3.3.5)

and (3.3.1) can be reformulated as

$$-\epsilon_\infty \Delta \Phi(\mathbf{r}) + (\epsilon_s - \epsilon_\infty)\Delta u(\mathbf{r}) + \bar{\kappa}^2 \Phi(\mathbf{r}) = \delta,$$

(3.3.6)

and further into

$$-\epsilon_\infty \Delta \Phi(\mathbf{r}) + \frac{\epsilon_s - \epsilon_\infty}{\lambda^2}(u(\mathbf{r}) - \Phi(\mathbf{r})) + \bar{\kappa}^2 \Phi(\mathbf{r}) = \delta.$$

(3.3.7)

Combining (3.3.5) and (3.3.7), we get a system of partial differential equations with respect to the unknown functions Φ and u as follows:

$$\begin{cases} -\epsilon_\infty \Delta \Phi(\mathbf{r}) + (\alpha_1 + \bar{\kappa}^2)\Phi(\mathbf{r}) - \alpha_1 u(\mathbf{r}) = \delta, & \mathbf{r} \in \mathbb{R}^3, \\ -\lambda^2 \Delta u(\mathbf{r}) + u(\mathbf{r}) - \Phi(\mathbf{r}) = 0, & \mathbf{r} \in \mathbb{R}^3, \\ \Phi(\mathbf{r}) \to 0, u(\mathbf{r}) \to 0 & \text{as } |\mathbf{r}| \to \infty, \end{cases}$$

(3.3.8)

where
$$\alpha_1 = \frac{\epsilon_s - \epsilon_\infty}{\lambda^2}.$$

Due to the property of spherical symmetry, it is easy to see that the solutions Φ and u must be radial functions in the sense that $\Phi(\mathbf{r}) = \Phi(|\mathbf{r}|)$ and $u(\mathbf{r}) = u(|\mathbf{r}|)$. Denoting $r = |\mathbf{r}|$, and changing the variable $\mathbf{r} = (x, y, z)$ into the spherical coordinates (r, θ, φ), we can reformulate (3.3.8) as the following second order ODE system:

$$\begin{cases} -\epsilon_\infty \dfrac{d^2}{dr^2}(r\Phi(r)) + (\alpha_1 + \bar{\kappa}^2)(r\Phi(r)) - \alpha_1(ru(r)) = 0, & r > 0, \\[2mm] -\lambda^2 \dfrac{d^2}{dr^2}(ru(r)) + ru(r) - r\Phi(r) = 0, & r > 0, \\[2mm] \Phi(r) \to 0, u(r) \to 0 & \text{as} \quad r \to \infty. \end{cases} \tag{3.3.9}$$

Setting $\bar{\Phi}(r) = r\Phi(r)$ and $\bar{u}(r) = ru(r)$, the above ODE system becomes

$$\begin{cases} -\epsilon_\infty \dfrac{d^2}{dr^2}(\bar{\Phi}(r)) + (\alpha_1 + \bar{\kappa}^2)(\bar{\Phi}(r)) - \alpha_1(\bar{u}(r)) = 0, & r > 0, \\[2mm] -\lambda^2 \dfrac{d^2}{dr^2}(\bar{u}(r)) + \bar{u}(r) - \bar{\Phi}(r) = 0, & r > 0, \end{cases} \tag{3.3.10}$$

or equivalently, in the matrix form

$$\frac{d^2}{dr^2}\begin{pmatrix} \bar{\Phi} \\ \bar{u} \end{pmatrix} = \begin{bmatrix} a_1 & -a_2 \\ -b & b \end{bmatrix}\begin{pmatrix} \bar{\Phi} \\ \bar{u} \end{pmatrix}, \tag{3.3.11}$$

where a_1, a_2, and b are defined by

$$a_1 = \frac{\alpha_1 + \bar{\kappa}^2}{\epsilon_\infty}, \quad a_2 = \frac{\alpha_1}{\epsilon_\infty}, \quad b = \frac{1}{\lambda^2}.$$

By direct calculations, the two eigenvalues of the coefficient matrix

$$\begin{bmatrix} a_1 & -a_2 \\ -b & b \end{bmatrix}$$

can be found respectively as

$$\omega_1 = \frac{1}{2}(a_1 + b + c), \qquad \omega_2 = \frac{1}{2}(a_1 + b - c), \tag{3.3.12}$$

and their corresponding eigenvectors ζ_1 and ζ_2 are:

$$\zeta_1 = \begin{pmatrix} 1 \\ \tau_1 \end{pmatrix}, \qquad \zeta_2 = \begin{pmatrix} 1 \\ \tau_{2,} \end{pmatrix}, \tag{3.3.13}$$

27

where c, τ_1, and τ_2 are defined by

$$c = \sqrt{(a_1 - b)^2 + 4a_2 b}, \quad \tau_1 = \frac{1}{2a_2}(a_1 - b - c), \quad \tau_2 = \frac{1}{2a_2}(a_1 - b + c).$$

Substituting the original notations to the above expressions, we get

$$
\begin{aligned}
\omega_1 &= \frac{\bar{\kappa}^2 \lambda^2 + \epsilon_s + \xi}{2\epsilon_\infty \lambda^2}, \quad \omega_2 = \frac{\bar{\kappa}^2 \lambda^2 + \epsilon_s - \xi}{2\epsilon_\infty \lambda^2}, \\
\tau_1 &= \frac{\bar{\kappa}^2 \lambda^2 + \epsilon_s - 2\epsilon_\infty - \xi}{2(\epsilon_s - \epsilon_\infty)}, \quad \tau_2 = \frac{\bar{\kappa}^2 \lambda^2 + \epsilon_s - 2\epsilon_\infty + \xi}{2(\epsilon_s - \epsilon_\infty)},
\end{aligned}
\tag{3.3.14}
$$

where ξ is defined by

$$\xi = \sqrt{(\bar{\kappa}^2 \lambda^2 + \epsilon_s)^2 - 4\epsilon_\infty \lambda^2 \bar{\kappa}^2}. \tag{3.3.15}$$

Lemma 3.3.1. *If $\epsilon_s \geq \epsilon_\infty$, then the eigenvalues ω_1 and ω_2 defined in (3.3.12) are two positive real numbers.*

Proof. Because a_1, a_2 and b are positive, c is a positive real number, thus ω_1 is positive. To prove $\omega_2 \geq 0$, by the equivalent form (3.3.14), it is sufficient to show that the numerator $\bar{\kappa}^2 \lambda^2 + \epsilon_s - \xi$ is positive. We first show that ξ is real: Suppose $\epsilon_s \geq \epsilon_\infty$ (which is reasonable in physics, e.g., when the solvent is water, under the room temperature, one has $\epsilon_s \approx 80$ and $\epsilon_\infty \approx 1.8$), the radicand of ξ can be factorized as

$$(\bar{\kappa}^2 \lambda^2 + \epsilon_s)^2 - 4\epsilon_\infty \lambda^2 \bar{\kappa}^2 = \left(\epsilon_s + \bar{\kappa}^2 \lambda^2 + 2\lambda \bar{\kappa} \sqrt{\epsilon_\infty}\right)\left(\epsilon_s + \bar{\kappa}^2 \lambda^2 - 2\lambda \bar{\kappa} \sqrt{\epsilon_\infty}\right),$$

it is easy to see that the first factor is positive, and the second factor satisfies

$$\epsilon_s + \bar{\kappa}^2 \lambda^2 - 2\lambda \bar{\kappa} \sqrt{\epsilon_\infty} \geq \epsilon_\infty + \bar{\kappa}^2 \lambda^2 - 2\lambda \bar{\kappa} \sqrt{\epsilon_\infty} = (\sqrt{\epsilon_\infty} - \bar{\kappa} \lambda)^2 \geq 0,$$

hence $\xi = \sqrt{(\bar{\kappa}^2 \lambda^2 + \epsilon_s)^2 - 4\epsilon_\infty \lambda^2 \bar{\kappa}^2}$ is real. Further, note that

$$(\bar{\kappa}^2 \lambda^2 + \epsilon_s)^2 > (\bar{\kappa}^2 \lambda^2 + \epsilon_s)^2 - 4\epsilon_\infty \bar{\kappa}^2 \lambda^2 = \xi^2$$

thus

$$\bar{\kappa}^2 \lambda^2 + \epsilon_s > \xi,$$

which implies that the numerator of ω_2 is positive. $\qquad\square$

Based on the results of Lemma 3.3.1, we have

28

Theorem 3.3.2. *The fundamental solution of PDE system* (3.3.8) *has the form*

$$\Phi(\mathbf{r}) = \frac{\tau_2}{4\pi\epsilon_\infty(\tau_2 - \tau_1)} \frac{e^{-\eta_1|\mathbf{r}|}}{|\mathbf{r}|} + \frac{\tau_1}{4\pi\epsilon_\infty(\tau_1 - \tau_2)} \frac{e^{-\eta_2|\mathbf{r}|}}{|\mathbf{r}|},$$

$$u(\mathbf{r}) = \frac{\tau_1\tau_2}{4\pi\epsilon_\infty(\tau_2 - \tau_1)} \frac{e^{-\eta_1|\mathbf{r}|}}{|\mathbf{r}|} + \frac{\tau_1\tau_2}{4\pi\epsilon_\infty(\tau_1 - \tau_2)} \frac{e^{-\eta_2|\mathbf{r}|}}{|\mathbf{r}|},$$

(3.3.16)

where

$$\eta_1 = \sqrt{\omega_1} = \frac{1}{\lambda}\sqrt{\frac{\bar{\kappa}^2\lambda^2 + \epsilon_s + \xi}{2\epsilon_\infty}}, \quad \eta_2 = \sqrt{\omega_2} = \frac{1}{\lambda}\sqrt{\frac{\bar{\kappa}^2\lambda^2 + \epsilon_s - \xi}{2\epsilon_\infty}}.$$

(3.3.17)

Proof. According to Lemma 3.3.1, η_1 and η_2 are two positive real numbers. Based on the classic ODE theory, the general solution of (3.3.11) can be written in the form

$$\bar{\Phi}(r) = c_1 e^{-\eta_1 r} + c_2 e^{-\eta_2 r} + c_3 e^{\eta_1 r} + c_4 e^{\eta_2 r},$$

$$\bar{u}(r) = c_1\tau_1 e^{-\eta_1 r} + c_2\tau_2 e^{-\eta_2 r} + c_3\tau_1 e^{\eta_1 r} + c_4\tau_2 e^{\eta_2 r},$$

which implies that the general solutions of (3.3.9) has the following form

$$\Phi(r) = c_1\frac{e^{-\eta_1 r}}{r} + c_2\frac{e^{-\eta_2 r}}{r} + c_3\frac{e^{\eta_1 r}}{r} + c_4\frac{e^{\eta_2 r}}{r},$$

(3.3.18)

$$u(r) = c_1\tau_1\frac{e^{-\eta_1 r}}{r} + c_2\tau_2\frac{e^{-\eta_2 r}}{r} + c_3\tau_1\frac{e^{\eta_1 r}}{r} + c_4\tau_2\frac{e^{\eta_2 r}}{r},$$

(3.3.19)

where c_1, c_2, c_3 and c_4 denote four constants to be determined.

By the boundary conditions $\Phi(r) \to 0$ and $u(r) \to 0$ as $r \to \infty$, it is easy to get that $c_3 = 0, c_4 = 0$. To determine the values of c_1 and c_2, two more conditions are needed. Because u is a smooth function in the whole space, we have

$$\lim_{r \to 0} ru(r) = 0,$$

(3.3.20)

from which we can obtain

$$c_1\tau_1 + c_2\tau_2 = 0.$$

(3.3.21)

The second condition can be obtained by integrating the both sides of the first equation of (3.3.8) over a small ball $B_\epsilon =: \{\mathbf{r} \mid |\mathbf{r}| \leq \epsilon\}$ centering at the origin with radius ϵ.

$$-\epsilon_\infty \int_{B_\epsilon} \Delta\Phi(\mathbf{r})d\mathbf{r} + (\alpha_1 + \bar{\kappa}^2) \int_{B_\epsilon} \Phi(\mathbf{r})d\mathbf{r} - \alpha_1 \int_{B_\epsilon} u(\mathbf{r})d\mathbf{r} = 1.$$

(3.3.22)

29

Here the property of the Dirac delta distribution δ has been used to get the right hand side of the above equation equal to 1.

Note that for a point $\mathbf{s} = (x, y, z)$ on the boundary of B_ϵ, its outward normal vector $\mathbf{n}(\mathbf{s}) = \frac{1}{\epsilon}(x, y, z)$ where $x^2 + y^2 + z^2 = \epsilon^2$. By the divergence theorem [18], we have

$$\int_{B_\epsilon} \Delta\Phi(\mathbf{r})\mathrm{d}\mathbf{r} = \int_{\partial B_\epsilon} \nabla\Phi(\mathbf{s}) \cdot \mathbf{n}(\mathbf{s})\mathrm{d}\mathbf{s} = \frac{1}{\epsilon}\int_{\partial B_\epsilon} (\Phi_x x + \Phi_y y + \Phi_z z)\mathrm{d}\mathbf{s}$$

$$= \int_{\partial B_\epsilon} \frac{\mathrm{d}\Phi(r)}{\mathrm{d}r}\mathrm{d}\mathbf{s} = \int_0^{2\pi}\int_0^\pi \frac{\mathrm{d}\Phi(\epsilon)}{\mathrm{d}r}\sin\phi\epsilon^2\mathrm{d}\phi\mathrm{d}\theta = 4\pi\epsilon^2\frac{\mathrm{d}\Phi(\epsilon)}{\mathrm{d}r}. \tag{3.3.23}$$

We then can calculate

$$\frac{\mathrm{d}\Phi(\epsilon)}{\mathrm{d}r} = \frac{\mathrm{d}}{\mathrm{d}r}\left(c_1\frac{e^{-\eta_1 r}}{r} + c_2\frac{e^{-\eta_2 r}}{r}\right)\bigg|_{r=\epsilon}$$

$$= \left(c_1\frac{-\eta_1 e^{-\eta_1 r}r - e^{-\eta_1 r}}{r^2} + c_2\frac{-\eta_2 e^{-\eta_2 r}r - e^{-\eta_2 r}}{r^2}\right)\bigg|_{r=\epsilon} \tag{3.3.24}$$

$$= c_1\frac{-\eta_1 e^{-\eta_1 \epsilon}\epsilon - e^{-\eta_1 \epsilon}}{\epsilon^2} + c_2\frac{-\eta_2 e^{-\eta_2 \epsilon}\epsilon - e^{-\eta_2 \epsilon}}{\epsilon^2}.$$

Hence, the first term of (3.3.22) can be evaluated as

$$-\epsilon_\infty \int_{B_\epsilon} \Delta\Phi(\mathbf{r})\mathrm{d}\mathbf{r} = -4\pi\epsilon_\infty[c_1(-\eta_1 e^{-\eta_1 \epsilon}\epsilon - e^{-\eta_1 \epsilon}) + c_2(-\eta_2 e^{-\eta_2 \epsilon}\epsilon - e^{-\eta_2 \epsilon})]. \tag{3.3.25}$$

Taking the limit as ϵ approaches to zero on both sides of (3.3.25), we get

$$\lim_{\epsilon \to 0}\left\{-\epsilon_\infty \int_{B_\epsilon} \Delta\Phi(\mathbf{r})\mathrm{d}\mathbf{r}\right\} = 4\pi\epsilon_\infty(c_1 + c_2).$$

For the second term of (3.3.22), we have

$$\int_{B_\epsilon} \Phi(\mathbf{r})\mathrm{d}\mathbf{r} = \int_{B_\epsilon}\left(c_1\frac{e^{-\eta_1|\mathbf{r}|}}{|\mathbf{r}|} + c_2\frac{e^{-\eta_2|\mathbf{r}|}}{|\mathbf{r}|}\right)\mathrm{d}\mathbf{r}$$

$$= c_1\int_0^{2\pi}\int_0^\pi\int_0^\epsilon \frac{e^{-\eta_1 r}}{r}r^2\sin\phi\mathrm{d}r\mathrm{d}\phi\mathrm{d}\theta + c_2\int_0^{2\pi}\int_0^\pi\int_0^\epsilon \frac{e^{-\eta_2 r}}{r}r^2\sin\phi\mathrm{d}r\mathrm{d}\phi\mathrm{d}\theta$$

$$= 4\pi c_1\int_0^\epsilon re^{-\eta_1 r}\mathrm{d}r + 4\pi c_2\int_0^\epsilon re^{-\eta_2 r}\mathrm{d}r.$$

Because the integrands are smooth functions, the above two integrals approach to 0 as ϵ approaches zero. This gives

$$\lim_{\epsilon \to 0}\int_{B_\epsilon} \Phi(\mathbf{r})\mathrm{d}\mathbf{r} = 0.$$

30

Similarly, we can show that

$$\lim_{\epsilon \to 0} \int_{B_\epsilon} u(\mathbf{r}) \mathrm{d}\mathbf{r} = 0.$$

Hence, letting ϵ approach to zero on the both sides of (3.3.22), we obtain the following equation as the second condition.

$$4\pi\epsilon_\infty(c_1 + c_2) = 1. \tag{3.3.26}$$

Combining (3.3.21) with (3.3.26) we get:

$$\begin{cases} c_1\tau_1 + c_2\tau_2 = 0, \\ 4\pi\epsilon_\infty(c_1 + c_2) = 1. \end{cases} \tag{3.3.27}$$

Solving the above algebraic system, we can find the values of c_1 and c_2 as follows:

$$c_1 = \frac{\tau_2}{4\pi\epsilon_\infty(\tau_2 - \tau_1)}, \qquad c_2 = \frac{\tau_1}{4\pi\epsilon_\infty(\tau_1 - \tau_2)}. \tag{3.3.28}$$

At last, according to (3.3.18), we substitute c_1 and c_2 by their values defined in (3.3.28), and use the fact $c_3 = c_4 = 0$, the fundamental solution of the ODE system (3.3.9) is found in the form of (3.3.16). $\qquad\square$

The analytical solution of the nonlocal Debye-Hückel equation (3.3.9) can be obtained by applying the superposition principle with respect to the multiple delta distribution $\{\delta_{\mathbf{r}_j}\}$. For clarity, we conclude our main results of this chapter as the following theorem.

Theorem 3.3.3. *The analytic solution of the nonlocal Debye-Hückel equation (3.2.6) has the form*

$$\begin{aligned}
\Phi(\mathbf{r}) =& \frac{\alpha\tau_2}{4\pi\epsilon_\infty(\tau_2 - \tau_1)} \sum_{j=1}^{n_p} z_j \frac{e^{-\eta_1|\mathbf{r}-\mathbf{r}_j|}}{|\mathbf{r}-\mathbf{r}_j|} + \frac{\alpha\tau_1}{4\pi\epsilon_\infty(\tau_1 - \tau_2)} \sum_{j=1}^{n_p} z_j \frac{e^{-\eta_2|\mathbf{r}-\mathbf{r}_j|}}{|\mathbf{r}-\mathbf{r}_j|} \\
=& \frac{\alpha}{4\pi\epsilon_\infty(\tau_2 - \tau_1)} \sum_{j=1}^{n_p} \frac{z_j}{|\mathbf{r}-\mathbf{r}_j|} \left(\tau_2 e^{-\eta_1|\mathbf{r}-\mathbf{r}_j|} - \tau_1 e^{-\eta_2|\mathbf{r}-\mathbf{r}_j|} \right), \\
u(\mathbf{r}) =& \frac{\alpha\tau_1\tau_2}{4\pi\epsilon_\infty(\tau_2 - \tau_1)} \sum_{j=1}^{n_p} z_j \frac{e^{-\eta_1|\mathbf{r}-\mathbf{r}_j|}}{|\mathbf{r}-\mathbf{r}_j|} + \frac{\alpha\tau_1\tau_2}{4\pi\epsilon_\infty(\tau_1 - \tau_2)} \sum_{j=1}^{n_p} z_j \frac{e^{-\eta_2|\mathbf{r}-\mathbf{r}_j|}}{|\mathbf{r}-\mathbf{r}_j|} \\
=& \frac{\alpha\tau_1\tau_2}{4\pi\epsilon_\infty(\tau_2 - \tau_1)} \sum_{j=1}^{n_p} \frac{z_j}{|\mathbf{r}-\mathbf{r}_j|} \left(e^{-\eta_1|\mathbf{r}-\mathbf{r}_j|} - e^{-\eta_2|\mathbf{r}-\mathbf{r}_j|} \right),
\end{aligned} \tag{3.3.29}$$

where $\mathbf{r} \in \mathbb{R}^3$ and $\mathbf{r} \neq \mathbf{r}_j$ for $j = 1, 2, \ldots, n_p$.

The nonlocal Debye-Hückel equation can be regarded as an extension of the traditional Debye-Hückel equation. The following corollary shows that the former can reduce to the latter as a limit case.

Corollary 3.3.4. *If $\bar{\kappa}^2\lambda^2 > \epsilon_s$, the solution of the nonlocal Debye-Hückel equation* (3.2.6) *includes the solution of the traditional Debye-Hückel equation* (3.1.25) *as a special case.*

Proof. We consider the limit case when ϵ_∞ approaches to ϵ_s. By (3.3.14) and (3.3.15),

$$\lim_{\epsilon_\infty \to \epsilon_s} \xi = \lim_{\epsilon_\infty \to \epsilon_s} \sqrt{(\bar{\kappa}^2\lambda^2 + \epsilon_s)^2 - 4\epsilon_\infty\lambda^2\bar{\kappa}^2} = \bar{\kappa}^2\lambda^2 - \epsilon_s,$$

and

$$\lim_{\epsilon_\infty \to \epsilon_s} \omega_1 = \lim_{\epsilon_\infty \to \epsilon_s} \frac{\bar{\kappa}^2\lambda^2 + \epsilon_s + \xi}{2\epsilon_\infty\lambda^2} = \frac{\bar{\kappa}^2}{\epsilon_s}, \quad \lim_{\epsilon_\infty \to \epsilon_s} \omega_2 = \lim_{\epsilon_\infty \to \epsilon_s} \frac{\bar{\kappa}^2\lambda^2 + \epsilon_s - \xi}{2\epsilon_\infty\lambda^2} = \frac{1}{\lambda^2},$$

$$\lim_{\epsilon_\infty \to \epsilon_s} \tau_1 = \lim_{\epsilon_\infty \to \epsilon_s} \frac{\bar{\kappa}^2\lambda^2 + \epsilon_s - 2\epsilon_\infty - \xi}{2(\epsilon_s - \epsilon_\infty)} = 1, \quad \lim_{\epsilon_\infty \to \epsilon_s} \tau_2 = \lim_{\epsilon_\infty \to \epsilon_s} \frac{\bar{\kappa}^2\lambda^2 + \epsilon_s - 2\epsilon_\infty + \xi}{2(\epsilon_s - \epsilon_\infty)} = \infty,$$

we get

$$\lim_{\epsilon_\infty \to \epsilon_s} \eta_1 = \lim_{\epsilon_\infty \to \epsilon_s} \sqrt{\omega_1} = \frac{\bar{\kappa}}{\sqrt{\epsilon_s}}, \quad \lim_{\epsilon_\infty \to \epsilon_s} \eta_2 = \lim_{\epsilon_\infty \to \epsilon_s} \sqrt{\omega_2} = \frac{1}{\lambda}.$$

Therefore, when ϵ_∞ approaches to ϵ_s, the solution Φ of the nonlocal Debye-Hückel equation becomes

$$
\begin{aligned}
&\lim_{\epsilon_\infty \to \epsilon_s} \Phi(\mathbf{r}) \\
&= \lim_{\epsilon_\infty \to \epsilon_s} \left(\frac{\alpha\tau_2}{4\pi\epsilon_\infty(\tau_2 - \tau_1)} \sum_{j=1}^{n_p} z_j \frac{e^{-\eta_1|\mathbf{r}-\mathbf{r}_j|}}{|\mathbf{r}-\mathbf{r}_j|} + \frac{\alpha\tau_1}{4\pi\epsilon_\infty(\tau_1 - \tau_2)} \sum_{j=1}^{n_p} z_j \frac{e^{-\eta_2|\mathbf{r}-\mathbf{r}_j|}}{|\mathbf{r}-\mathbf{r}_j|} \right) \\
&= \lim_{\epsilon_\infty \to \epsilon_s} \left(\frac{\alpha}{4\pi\epsilon_\infty\left(1 - \frac{\tau_1}{\tau_2}\right)} \sum_{j=1}^{n_p} z_j \frac{e^{-\eta_1|\mathbf{r}-\mathbf{r}_j|}}{|\mathbf{r}-\mathbf{r}_j|} + \frac{\alpha\tau_1}{4\pi\epsilon_\infty(\tau_1 - \tau_2)} \sum_{j=1}^{n_p} z_j \frac{e^{-\eta_2|\mathbf{r}-\mathbf{r}_j|}}{|\mathbf{r}-\mathbf{r}_j|} \right) \quad (3.3.30) \\
&= \frac{\alpha}{4\pi\epsilon_s} \sum_{j=1}^{n_p} \frac{z_j}{|\mathbf{r}-\mathbf{r}_j|} e^{-\frac{\bar{\kappa}}{\sqrt{\epsilon_s}}|\mathbf{r}-\mathbf{r}_j|},
\end{aligned}
$$

which is exactly the solution of the local Debye-Hückel equation as shown in (3.1.26). Mean-

while, the auxiliary function u becomes:

$$\lim_{\epsilon_\infty \to \epsilon_s} u(\mathbf{r})$$

$$= \lim_{\epsilon_\infty \to \epsilon_s} \frac{\alpha \tau_1 \tau_2}{4\pi\epsilon_\infty(\tau_2 - \tau_1)} \sum_{j=1}^{n_p} \frac{z_j}{|\mathbf{r} - \mathbf{r}_j|} \left(e^{-\eta_1|\mathbf{r}-\mathbf{r}_j|} - e^{-\eta_2|\mathbf{r}-\mathbf{r}_j|} \right)$$

$$= \lim_{\epsilon_\infty \to \epsilon_s} \frac{\alpha \tau_1}{4\pi\epsilon_\infty \left(1 - \frac{\tau_1}{\tau_2}\right)} \sum_{j=1}^{n_p} \frac{z_j}{|\mathbf{r} - \mathbf{r}_j|} \left(e^{-\eta_1|\mathbf{r}-\mathbf{r}_j|} - e^{-\eta_2|\mathbf{r}-\mathbf{r}_j|} \right) \qquad (3.3.31)$$

$$= \frac{\alpha}{4\pi\epsilon_s} \sum_{j=1}^{n_p} \frac{z_j}{|\mathbf{r} - \mathbf{r}_j|} \left(e^{-\frac{\bar{\kappa}}{\sqrt{\epsilon_s}}|\mathbf{r}-\mathbf{r}_j|} - e^{-\frac{1}{\lambda}|\mathbf{r}-\mathbf{r}_j|} \right).$$

$\square$

3.4 A solution decomposition scheme

The Dirac delta distributions bring strong singularities in the nonlocal Debye-Huckel equations, which induces difficulties in analyzing and solving these equations. In this section, similar to the case of PBE, we propose a solution decomposition scheme to deal with this issue.

Clearly, setting $u = \Phi * Q_\lambda$, we can formulate (3.2.5) as a system of two PDEs:

$$\begin{cases} -\epsilon_\infty \Delta \Phi(\mathbf{r}) + \dfrac{\epsilon_s - \epsilon_\infty}{\lambda^2} \Big(\Phi(\mathbf{r}) - u(\mathbf{r}) \Big) + \dfrac{2Me^2}{\epsilon_0 k_B T} \sinh \big(\Phi(\mathbf{r}) \big) \\ \qquad\qquad = \dfrac{e_c^2}{\epsilon_0 k_B T} \displaystyle\sum_{j=1}^{n_p} z_j \delta_{\mathbf{r}_j}, & \mathbf{r} \in \mathbb{R}^3, \\ -\lambda^2 \Delta u(\mathbf{r}) + u(\mathbf{r}) - \Phi(\mathbf{r}) = 0, & \mathbf{r} \in \mathbb{R}^3, \\ \qquad\qquad \Phi(\mathbf{r}) \to 0 & \text{as} \quad |\mathbf{r}| \to \infty. \end{cases} \qquad (3.4.1)$$

We decompose the solution Φ and u of (3.4.1) as follows

$$\Phi(\mathbf{r}) = \Psi(\mathbf{r}) + G(\mathbf{r}), \qquad \text{and} \qquad u = u_0 + u_1, \qquad (3.4.2)$$

where G is given as

$$G(\mathbf{r}) = \frac{\alpha}{4\pi\epsilon_\infty} \sum_{j=1}^{n_p} \frac{z_j}{|\mathbf{r} - \mathbf{r}_j|} \qquad (3.4.3)$$

33

$u_0 = G * Q_\lambda$, which can be found as [76]:

$$u_0(\mathbf{r}) = \frac{\alpha}{4\pi\epsilon_\infty} \sum_{j=1}^{n_p} z_j \frac{1 - e^{-|\mathbf{r}-\mathbf{r}_j|/\lambda}}{|\mathbf{r} - \mathbf{r}_j|}, \tag{3.4.4}$$

and $u_1 = \Psi * Q_\lambda$.

From (3.4.1), it can be found that Ψ and u_1 satisfy the following PDE system

$$\begin{cases} -\epsilon_\infty \Delta\Psi(\mathbf{r}) + \dfrac{\epsilon_s - \epsilon_\infty}{\lambda^2}\Big(\Psi(\mathbf{r}) - u_1(\mathbf{r})\Big) \\ \quad + \dfrac{2Me^2}{\epsilon_0 k_B T} \sinh\big(\Psi(\mathbf{r}) + G(\mathbf{r})\big) = \dfrac{\epsilon_\infty - \epsilon_s}{\lambda^2}\Big(G(\mathbf{r}) - u_0(\mathbf{r})\Big), & \mathbf{r} \in \mathbb{R}^3, \\ -\lambda^2 \Delta u_1(\mathbf{r}) + u_1(\mathbf{r}) - \Psi(\mathbf{r}) = 0, & \mathbf{r} \in \mathbb{R}^3, \\ \Psi(\mathbf{r}) \to 0, u_1(\mathbf{r}) \to 0 & \text{as} \quad |\mathbf{r}| \to \infty. \end{cases} \tag{3.4.5}$$

As a linear case of (3.4.5), we find that Ψ and u_1 satisfy the following system of linear PDEs:

$$\begin{cases} -\epsilon_\infty \Delta\Psi(\mathbf{r}) + (\alpha_1 + \bar{\kappa}^2)\Psi(\mathbf{r}) - \alpha_1 u_1(\mathbf{r}) \\ \quad = -(\alpha_1 + \bar{\kappa}^2)G(\mathbf{r}) + \alpha_1 u_0(\mathbf{r}), & \mathbf{r} \in \mathbb{R}^3, \\ -\lambda^2 \Delta u_1(\mathbf{r}) + u_1(\mathbf{r}) - \Psi(\mathbf{r}) = 0, & \mathbf{r} \in \mathbb{R}^3, \\ \Psi(\mathbf{r}) \to 0, \quad u_1(\mathbf{r}) \to 0 & \text{as} \quad |\mathbf{r}| \to \infty. \end{cases} \tag{3.4.6}$$

Using the analytical expression of Φ and u given in (3.3.29), we can obtain the analytical expressions of Ψ and u_1 as follows:

$$\begin{cases} \Psi(\mathbf{r}) \equiv \dfrac{\alpha}{4\pi\epsilon_\infty} \sum_{j=1}^{n_p} z_j \left(\dfrac{\tau_2}{\tau_2 - \tau_1} \dfrac{e^{-\eta_1|\mathbf{r}-\mathbf{r}_j|}}{|\mathbf{r}-\mathbf{r}_j|} + \dfrac{\tau_1}{\tau_1 - \tau_2} \dfrac{e^{-\eta_2|\mathbf{r}-\mathbf{r}_j|}}{|\mathbf{r}-\mathbf{r}_j|} - \dfrac{1}{|\mathbf{r}-\mathbf{r}_j|} \right) \\ \qquad = \dfrac{\alpha}{4\pi\epsilon_\infty(\tau_2 - \tau_1)} \sum_{j=1}^{n_p} z_j \dfrac{\tau_2 e^{-\eta_1|\mathbf{r}-\mathbf{r}_j|} - \tau_1 e^{-\eta_2|\mathbf{r}-\mathbf{r}_j|} - (\tau_2 - \tau_1)}{|\mathbf{r}-\mathbf{r}_j|}, \\ u_1(\mathbf{r}) \equiv \dfrac{\alpha}{4\pi\epsilon_\infty} \sum_{j=1}^{n_p} z_j \left(\dfrac{\tau_1\tau_2}{\tau_2 - \tau_1} \dfrac{e^{-\eta_1|\mathbf{r}-\mathbf{r}_j|}}{|\mathbf{r}-\mathbf{r}_j|} + \dfrac{\tau_1\tau_2}{\tau_1 - \tau_2} \dfrac{e^{-\eta_2|\mathbf{r}-\mathbf{r}_j|}}{|\mathbf{r}-\mathbf{r}_j|} - \dfrac{1 - e^{-|\mathbf{r}-\mathbf{r}_j|/\lambda}}{|\mathbf{r}-\mathbf{r}_j|} \right) \\ \qquad = \dfrac{\alpha}{4\pi\epsilon_\infty(\tau_2 - \tau_1)} \sum_{j=1}^{n_p} z_j \dfrac{\tau_1\tau_2 (e^{-\eta_1|\mathbf{r}-\mathbf{r}_j|} - e^{-\eta_2|\mathbf{r}-\mathbf{r}_j|}) - (\tau_2 - \tau_1)(1 - e^{-|\mathbf{r}-\mathbf{r}_j|/\lambda})}{|\mathbf{r}-\mathbf{r}_j|}. \end{cases}$$
$$\tag{3.4.7}$$

Remark 3.4.1. Clearly, Ψ and u_1 have potential singular terms at $\mathbf{r} = \mathbf{r}_i$ in their terms

$$\Psi_i = \frac{\alpha z_i}{4\pi\epsilon_\infty(\tau_2 - \tau_1)} \frac{\tau_2 e^{-\eta_1|\mathbf{r}-\mathbf{r}_i|} - \tau_1 e^{-\eta_2|\mathbf{r}-\mathbf{r}_i|} - (\tau_2 - \tau_1)}{|\mathbf{r}-\mathbf{r}_i|},$$

and
$$u_{1,i} = \frac{\alpha z_i}{4\pi\epsilon_\infty(\tau_2 - \tau_1)} \frac{\tau_1\tau_2(e^{-\eta_1|\mathbf{r}-\mathbf{r}_i|} - e^{-\eta_2|\mathbf{r}-\mathbf{r}_i|}) - (\tau_2 - \tau_1)(1 - e^{-|\mathbf{r}-\mathbf{r}_i|/\lambda})}{|\mathbf{r} - \mathbf{r}_i|}.$$

By L'Hôpital's law, their limits can be found as follows:

$$\lim_{|\mathbf{r}-\mathbf{r}_i|\to 0} \frac{\tau_2 e^{-\eta_1|\mathbf{r}|} - \tau_1 e^{-\eta_2|\mathbf{r}|} - (\tau_2 - \tau_1)}{|\mathbf{r}|}$$
$$= \lim_{|\mathbf{r}-\mathbf{r}_i|\to 0} -\tau_2\eta_1 e^{-\eta_1|\mathbf{r}|} + \tau_1\eta_2 e^{-\eta_2|\mathbf{r}|} = \tau_1\eta_2 - \tau_2\eta_1$$

and

$$\lim_{|\mathbf{r}-\mathbf{r}_i|\to 0} \frac{\tau_1\tau_2(e^{-\eta_1|\mathbf{r}|} - e^{-\eta_2|\mathbf{r}|}) - (\tau_2 - \tau_1)(1 - e^{-|\mathbf{r}|/\lambda})}{|\mathbf{r}|}$$
$$= \lim_{|\mathbf{r}-\mathbf{r}_i|\to 0} \left(\tau_1\tau_2(-\eta_1 e^{-\eta_1|\mathbf{r}|} + \eta_2 e^{-\eta_2|\mathbf{r}|}) - \frac{\tau_2 - \tau_1}{\lambda}e^{-|\mathbf{r}|/\lambda}\right)$$
$$= \tau_1\tau_2(\eta_2 - \eta_1) - \frac{\tau_2 - \tau_1}{\lambda}.$$

Hence,

$$\lim_{|\mathbf{r}-\mathbf{r}_i|\to 0} \Psi_i(\mathbf{r}) = \frac{\alpha z_i(\tau_1\eta_2 - \tau_2\eta_1)}{4\pi\epsilon_\infty(\tau_2 - \tau_1)},$$

and

$$\lim_{|\mathbf{r}-\mathbf{r}_i|\to 0} u_{1,i}(\mathbf{r}) = \frac{\alpha z_i}{4\pi\epsilon_\infty(\tau_2 - \tau_1)}\left(\tau_1\tau_2(\eta_2 - \eta_1) - \frac{\tau_2 - \tau_1}{\lambda}\right). \tag{3.4.8}$$

This shows that the singular points $\mathbf{r}_i$ for $i = 1, 2, \ldots, n$ of Ψ and u_1 are removable.

Chapter 4

Nonlocal Linearized Poisson-Boltzmann Equations

As introduced in Chapter 2, Poisson-Boltzmann equation can be used to predict the electrostatic potential distributions in a dielectric system in which a biomolecule is immersed in an electrolyte. However, the classic PB theory ignores all interactions among solvent molecules, and may cause a significant inaccuracy in the area that is exposed to a strong electrostatic field. In this chapter, we will investigate several electrostatics dielectric models that combine the PB theory and the nonlocal dielectric modeling scheme, as well as linearization techniques.

4.1 A nonlocal nonlinear Poisson-Boltzmann equation

First, we derive a nonlocal linear Poisson-Boltzmann equation based on the traditional linearization approach.

Here, we use the same setting as the one for PBE, as given in section 2.2. That is, the whole space $\mathbb{R}^3$ is composed of two open domains D_p, D_s and their interface Γ.

$$\mathbb{R}^3 = D_p \cup D_s \cup \Gamma, \tag{4.1.1}$$

such that D_p is surrounded by D_s.

The solute domain D_p is supposed to hold a protein composed of n_p atoms as fixed point charges. The j-th atom centers at $\mathbf{r}_j$ and carries $z_j e_c$ charge quantities. Besides, D_p and is regarded as a uniform dielectric material with dielectric constant ϵ_p. In D_p, the electrostatic

potential Φ satisfies the Poisson equation:

$$-\epsilon_p \Delta \Phi(\mathbf{r}) = \frac{e_c^2}{\epsilon_0 k_B T} \sum_{j=1}^{n_p} z_j \delta_{\mathbf{r}_j}, \qquad \mathbf{r} \in D_p. \tag{4.1.2}$$

On the other hand, there are n species of ions dissolved in the solvent domain D_s. The electrostatic potential Φ satisfies the following nonlocal Poisson equation:

$$
\begin{aligned}
-\nabla \cdot \left(\epsilon_\infty \nabla \Phi(\mathbf{r}) + (\epsilon_s - \epsilon_\infty) \nabla \int_{\mathbb{R}^3} \frac{e^{-|\mathbf{r}-\mathbf{r}'|/\lambda}}{4\pi\lambda^2 |\mathbf{r}-\mathbf{r}'|} \Phi(\mathbf{r}') d\mathbf{r}' \right) \\
= \frac{e_c^2}{\epsilon_0 k_B T} \sum_{i=1}^{n} Z_i M_i e^{-Z_i \Phi(\mathbf{r})}, \qquad \mathbf{r} \in D_s.
\end{aligned}
\tag{4.1.3}
$$

Similar to the case of PBE, the interface conditions of the above equation can be induced due to the fact that the electrostatic potential Φ and the flux of the displacement field $\mathbf{D}$ are continuous across Γ.

$$\lim_{\mu \to 0^+} \Phi(\mathbf{s} - \mu\mathbf{n}(\mathbf{s})) = \lim_{\mu \to 0^+} \Phi(\mathbf{s} + \mu\mathbf{n}(\mathbf{s})), \qquad \mathbf{s} \in \Gamma, \tag{4.1.4}$$

and

$$\lim_{\mu \to 0^+} \mathbf{D}(\mathbf{s} - \mu\mathbf{n}(\mathbf{s})) \cdot \mathbf{n}(\mathbf{s}) = \lim_{\mu \to 0^+} \mathbf{D}(\mathbf{s} + \mu\mathbf{n}(\mathbf{s})) \cdot \mathbf{n}(\mathbf{s}), \qquad \mathbf{s} \in \Gamma, \tag{4.1.5}$$

where $n(\mathbf{s})$ is the outward unit normal vector at $\mathbf{s}$ on the interface Γ.

Note that

$$\lim_{\mu \to 0^+} \mathbf{D}(\mathbf{s} - \mu\mathbf{n}(\mathbf{s})) \cdot \mathbf{n}(\mathbf{s}) = \lim_{\mu \to 0^+} \epsilon_p \nabla \Phi(\mathbf{s} - \mu\mathbf{n}(\mathbf{s})) \cdot \mathbf{n}(\mathbf{s}), \tag{4.1.6}$$

and

$$
\begin{aligned}
&\lim_{\mu \to 0^+} \mathbf{D}(\mathbf{s} + \mu\mathbf{n}(\mathbf{s})) \cdot \mathbf{n}(\mathbf{s}) \\
&= \lim_{\mu \to 0^+} \left(\epsilon_\infty \nabla \Phi(\mathbf{s} + \mu\mathbf{n}(\mathbf{s})) + (\epsilon_s - \epsilon_\infty) \nabla \int_{\mathbb{R}^3} \frac{e^{-|\mathbf{s}+\mu\mathbf{n}(\mathbf{s})-\mathbf{r}'|/\lambda}}{4\pi\lambda^2 |\mathbf{s}+\mu\mathbf{n}(\mathbf{s})-\mathbf{r}'|} \Phi(\mathbf{r}') d\mathbf{r}' \right) \cdot \mathbf{n}(\mathbf{s}).
\end{aligned}
\tag{4.1.7}
$$

Hence, by (4.1.5), the nonlocal flux continuity condition can be obtained as follows:

$$\epsilon_p \frac{\partial \Phi(\mathbf{s}^-)}{\partial \mathbf{n}(\mathbf{s})} = \epsilon_\infty \frac{\partial \Phi(\mathbf{s}^+)}{\partial \mathbf{n}(\mathbf{s})} + (\epsilon_s - \epsilon_\infty) \frac{\partial (\Phi * Q_\lambda)(\mathbf{s}^+)}{\partial \mathbf{n}(\mathbf{s})}. \tag{4.1.8}$$

Here, the convolution kernel Q_λ is defined in (3.2.2).

37

For clarity, we now write the nonlocal nonlinear Poisson-Boltzmann equation as the following interface problem:

$$
\begin{cases}
-\epsilon_p \Delta \Phi(\mathbf{r}) = \dfrac{e_c^2}{\epsilon_0 k_B T} \sum_{j=1}^{n_p} z_j \delta_{\mathbf{r}_j}, & \mathbf{r} \in D_p, \\[2ex]
-\nabla \cdot \Big(\epsilon_\infty \nabla \Phi(\mathbf{r}) + (\epsilon_s - \epsilon_\infty) \nabla (Q_\lambda * \Phi)(\mathbf{r}) \Big) \\[1ex]
\qquad\qquad - \dfrac{e_c^2}{\epsilon_0 k_B T} \sum_{i=1}^{n} Z_i M_i e^{-Z_i \Phi(\mathbf{r})} = 0, & \mathbf{r} \in D_s, \\[2ex]
\Phi(\mathbf{s}^-) = \Phi(\mathbf{s}^+), & \mathbf{s} \in \Gamma, \\[2ex]
\epsilon_p \dfrac{\partial \Phi(\mathbf{s}^-)}{\partial \mathbf{n}(\mathbf{s})} = \epsilon_\infty \dfrac{\partial \Phi(\mathbf{s}^+)}{\partial \mathbf{n}(\mathbf{s})} + (\epsilon_s - \epsilon_\infty) \dfrac{\partial (\Phi * Q_\lambda)(\mathbf{s}^+)}{\partial \mathbf{n}(\mathbf{s})}, & \mathbf{s} \in \Gamma, \\[2ex]
\Phi(\mathbf{r}) \to 0 & \text{as} \quad |\mathbf{r}| \to \infty.
\end{cases}
\tag{4.1.9}
$$

In particular, for the typical 1:1 symmetric ionic solution case ($n = 2, M_1 = M_2 = M, z_1 = 1$ and $z_2 = -1$), the second equation of (4.1.9) for the solvent domain D_s can be simplified into

$$
-\nabla \cdot \Big(\epsilon_\infty \nabla \Phi(\mathbf{r}) + (\epsilon_s - \epsilon_\infty) \nabla (Q_\lambda * \Phi)(\mathbf{r}) \Big) + \frac{2 M e_c^2}{\epsilon_0 k_B T} \sinh(\Phi(\mathbf{r})) = 0 \qquad \mathbf{r} \in D_s. \tag{4.1.10}
$$

As the traditional local PBE, we can also apply a decomposition scheme to split the solution of the nonlocal PBE into three components. In fact, we have the following theorem (see [33]):

Theorem 4.1.1. *The solutions Φ and u of the nonlocal Poisson Boltzmann model (4.1.9) have the following splitting formulas:*

$$
\Phi(\mathbf{r}) = \tilde{\Phi}(\mathbf{r}) + \Psi(\mathbf{r}) + G(\mathbf{r}), \tag{4.1.11}
$$

where G is defined by

$$
G(\mathbf{r}) = \frac{e_c^2}{4 \pi \epsilon_0 \epsilon_p k_B T} \sum_{j=1}^{n_p} \frac{z_j}{|\mathbf{r} - \mathbf{r}_j|}, \qquad \mathbf{r} \in \mathbb{R}^3, \tag{4.1.12}
$$

Ψ satisfies

$$
\begin{cases}
\Delta \Psi(\mathbf{r}) = 0, & \mathbf{r} \in D_p, \\[2ex]
-\nabla \cdot \Big(\epsilon_\infty \nabla \Psi(\mathbf{r}) + (\epsilon_s - \epsilon_\infty) \nabla (Q_\lambda * \Psi)(\mathbf{r}) \Big) \\[1ex]
\qquad\qquad = (\epsilon_\infty - \epsilon_s) \Delta (Q_\lambda * G)(\mathbf{r}), & \mathbf{r} \in D_s,
\end{cases}
\tag{4.1.13}
$$

38

with boundary conditions

$$\Psi(\mathbf{r}) \to 0 \qquad \text{as} \quad |\mathbf{r}| \to \infty, \tag{4.1.14}$$

and interface conditions

$$\begin{cases} \Psi(\mathbf{s}^-) = \Psi(\mathbf{s}^+), & \mathbf{s} \in \Gamma, \\ \epsilon_p \dfrac{\partial \Psi(\mathbf{s}^-)}{\partial \mathbf{n}(\mathbf{s})} = \epsilon_\infty \dfrac{\partial \Psi(\mathbf{s}^+)}{\partial \mathbf{n}(\mathbf{s})} + (\epsilon_s - \epsilon_\infty) \dfrac{\partial(Q_\lambda * \Psi)(\mathbf{s})}{\partial \mathbf{n}(\mathbf{s})} \\ \quad + (\epsilon_s - \epsilon_\infty) \dfrac{\partial(Q_\lambda * G)(\mathbf{s})}{\partial \mathbf{n}(\mathbf{s})} + (\epsilon_\infty - \epsilon_p) \dfrac{\partial G(\mathbf{s})}{\partial \mathbf{n}(\mathbf{s})}, & \mathbf{s} \in \Gamma, \end{cases} \tag{4.1.15}$$

and $\tilde{\Phi}$ *satisfies the following nonlinear equation*

$$\begin{cases} \Delta \tilde{\Phi}(\mathbf{r}) = 0, & \mathbf{r} \in D_p, \\ -\nabla \cdot \left(\epsilon_\infty \nabla \tilde{\Phi}(\mathbf{r}) + (\epsilon_s - \epsilon_\infty) \nabla(Q_\lambda * \tilde{\Phi})(\mathbf{r}) \right) \\ \quad = \dfrac{e_c^2}{\epsilon_0 k_B T} \displaystyle\sum_{i=1}^{n} z_i M_i e^{-\beta e_c z_i [\tilde{\Phi}(\mathbf{r}) + \Psi(\mathbf{r}) + G(\mathbf{r})]}, & \mathbf{r} \in D_s, \end{cases} \tag{4.1.16}$$

with boundary conditions

$$\tilde{\Phi}(\mathbf{r}) \to 0 \qquad \text{as} \quad |\mathbf{r}| \to \infty, \tag{4.1.17}$$

and interface conditions

$$\begin{cases} \tilde{\Phi}(\mathbf{s}^-) = \tilde{\Phi}(\mathbf{s}^+), & \mathbf{s} \in \Gamma, \\ \epsilon_p \dfrac{\partial \tilde{\Phi}(\mathbf{s}^-)}{\partial \mathbf{n}(\mathbf{s})} = \epsilon_\infty \dfrac{\partial \tilde{\Phi}(\mathbf{s}^+)}{\partial \mathbf{n}(\mathbf{s})} + (\epsilon_s - \epsilon_\infty) \dfrac{\partial(Q_\lambda * \tilde{\Phi})(\mathbf{s})}{\partial \mathbf{n}(\mathbf{s})}, & \mathbf{s} \in \Gamma. \end{cases} \tag{4.1.18}$$

4.2 Linearizations

The highly nonlinear Boltzmann term $\sum_{i=1}^{n} M_i e^{-Z_i \Phi(\mathbf{r})}$ for ionic concentrations has been used to construct several dielectric continuum models including PBE, our nonlinear Debye-Hückel equation, and our nonlocal PBE, but it induces difficulties in numerical calculations and theoretical analysis. Due to this reason, it is often linearized to yield simplified linear models.

4.2.1 Traditional approach

Traditionally, the Boltzmann term is linearized by using the taylor expansion of exponential function $f(x) = e^x$, at $x = 0$:

$$e^x = 1 + x + \frac{x^2}{2!} + \cdots + \frac{x^n}{n!} + \cdots$$

If the magnitude $|x|$ is sufficiently small, e^x can be approximated as

$$e^x \approx 1 + x \qquad \text{for} \qquad |x| \ll 1. \tag{4.2.1}$$

Note that $Z_i\Phi(\mathbf{r})$ is a real number at each position $\mathbf{r} \in D_s$. If $|Z_i\Phi(\mathbf{r})| \ll 1$, then by (4.2.1), the Boltzmann term has the linearization approximation

$$
\begin{aligned}
&\sum_{i=1}^{n} Z_i M_i e^{-Z_i\Phi(\mathbf{r})} \\
&\approx \sum_{i=1}^{n} Z_i M_i (1 - Z_i\Phi(\mathbf{r})) \\
&= \sum_{i=1}^{n} Z_i M_i - \sum_{i=1}^{n} Z_i^2 M_i \Phi(\mathbf{r}) \\
&= - \sum_{i=1}^{n} Z_i^2 M_i \Phi(\mathbf{r}).
\end{aligned}
\tag{4.2.2}
$$

Here we have assumed that the ionic solution is electroneutral:

$$\sum_{i=1}^{n} Z_i M_i = 0. \tag{4.2.3}$$

In particular, for the symmetric $1:1$ ionic solution, we have $M_1 = M_2 = M$, $Z_1 = 1$ and $Z_2 = -1$, the linearization can be performed as

$$\sum_{i=1}^{2} Z_i M e^{-Z_i\Phi(\mathbf{r})} = 2M\sinh(\Phi(\mathbf{r})) \approx 2M\Phi(\mathbf{r}). \tag{4.2.4}$$

Applying (4.2.2) to the second equation of (4.1.9), we can get a nonlocal linearized Poisson-Boltzmann equation as follows:

$$
\begin{cases}
-\epsilon_p \Delta\Phi(\mathbf{r}) = \dfrac{e_c^2}{\epsilon_0 k_B T} \displaystyle\sum_{j=1}^{n_p} z_j \delta_{\mathbf{r}_j}, & \mathbf{r} \in D_p, \\[2ex]
-\nabla \cdot \left(\epsilon_\infty \nabla\Phi(\mathbf{r}) + (\epsilon_s - \epsilon_\infty)\nabla(Q_\lambda * \Phi)(\mathbf{r}) \right) + \dfrac{e_c^2}{\epsilon_0 k_B T} \displaystyle\sum_{i=1}^{n} Z_i^2 M_i \Phi(\mathbf{r}) = 0, & \mathbf{r} \in D_s.
\end{cases}
\tag{4.2.5}
$$

The above equation satisfies the interface conditions and the boundary conditions in the same form of (4.1.9).

Inevitably, this linearization will introduce errors in searching for the electrostatic potential Φ. To keep an acceptable accuracy, the potential magnitude $|\Phi(\mathbf{r})|$ must be small enough for all $\mathbf{r}$ in the solvent domain D_s. In practice, this usually indicates that the ionic strength of solution is low enough.

4.2.2 A new linearization scheme

To improve the accuracy of the linear model (4.2.5), in this section, we introduce a new linear model using the solution splitting formula given in Theorem 4.1.1. According to this solution decomposition, we can first calculate G by using formula (4.1.12), and find Ψ by solving a linear problem (4.1.13). We then can use G and Ψ as given functions when we calculate $\tilde{\Phi}$ by solving the nonlinear problem (4.1.16). Hence, instead of linearizing the Boltzmann term with respect to Φ, we can linearize (4.1.16) with respect to the component $\tilde{\Phi}$. This solution decomposition scheme motivates us to propose a new strategy for linearizing the nonlocal PBE.

Proposition 4.2.1. *In the same settings as Theorem* (4.1.1), *suppose G and Ψ are pre-calculated, and $|\tilde{\Phi}|$ is small enough, the Boltzmann term can be linearized by*

$$\sum_{i=1}^{n} Z_i M_i e^{-Z_i \Phi(\mathbf{r})} \approx A_1(\mathbf{r}) + B_1(\mathbf{r})\tilde{\Phi}(\mathbf{r}) \qquad \mathbf{r} \in D_s, \tag{4.2.6}$$

where function A_1 and B_1 are defined by

$$A_1(\mathbf{r}) = \sum_{i=1}^{n} Z_i M_i e^{-Z_i[G(\mathbf{r})+\Psi(\mathbf{r})]} \tag{4.2.7}$$

and

$$B_1(\mathbf{r}) = \sum_{i=1}^{n} -Z_i^2 M_i e^{-Z_i[G(\mathbf{r})+\Psi(\mathbf{r})]} \tag{4.2.8}$$

Proof. The proof is straight forward. By $\Phi = G + \Psi + \tilde{\Phi}$, we have

$$\sum_{i=1}^{n} Z_i M_i e^{-Z_i \Phi(\mathbf{r})}$$

$$= \sum_{i=1}^{n} Z_i M_i e^{-Z_i [G(\mathbf{r}) + \Psi(\mathbf{r}) + \tilde{\Phi}(\mathbf{r})]} \tag{4.2.9}$$

$$= \sum_{i=1}^{n} Z_i M_i e^{-Z_i [G(\mathbf{r}) + \Psi(\mathbf{r})]} e^{-Z_i \tilde{\Phi}(\mathbf{r})}.$$

If $|\tilde{\Phi}(\mathbf{r})| \ll 1$ for all $\mathbf{r} \in D_s$, then for each i, we can approximate $e^{-Z_i \tilde{\Phi}(\mathbf{r})}$ by

$$e^{-Z_i \tilde{\Phi}(\mathbf{r})} \approx \left(1 - Z_i \tilde{\Phi}(\mathbf{r})\right). \tag{4.2.10}$$

Accordingly,

$$\sum_{i=1}^{n} Z_i M_i e^{-Z_i [G(\mathbf{r}) + \Psi(\mathbf{r})]} e^{-Z_i \tilde{\Phi}(\mathbf{r})}$$

$$\approx \sum_{i=1}^{n} Z_i M_i e^{-Z_i [G(\mathbf{r}) + \Psi(\mathbf{r})]} \left(1 - Z_i \tilde{\Phi}(\mathbf{r})\right) \tag{4.2.11}$$

$$= \sum_{i=1}^{n} \left(Z_i M_i e^{-Z_i [G(\mathbf{r}) + \Psi(\mathbf{r})]}\right) - \sum_{i=1}^{n} \left(Z_i^2 M_i e^{-Z_i [G(\mathbf{r}) + \Psi(\mathbf{r})]}\right) \tilde{\Phi}(\mathbf{r})$$

$$= A_1(\mathbf{r}) + B_1(\mathbf{r}) \tilde{\Phi}(\mathbf{r}).$$

This proves the proposition. $\qquad \square$

Remark 4.2.2. For the symmetric 1:1 symmetric ionic solution, the linearization can be performed as

$$\sinh(\Phi(\mathbf{r}))$$

$$= \sinh(G(\mathbf{r}) + \Psi(\mathbf{r}) + \tilde{\Phi}(\mathbf{r})) \tag{4.2.12}$$

$$\approx \sinh(G(\mathbf{r}) + \Psi(\mathbf{r})) + \cosh(G(\mathbf{r}) + \Psi(\mathbf{r})) \tilde{\Phi}(\mathbf{r}), \qquad \forall \mathbf{r} \in D_s.$$

Applying (4.2.6) into the second equation of (4.1.16), we get a new linear nonlocal Poisson-Boltzmann equation defined via solution solution decomposition $\Phi = G + \Psi + \tilde{\Phi}$, where G is defined in (4.1.12), Ψ is the solution of (4.1.13), and $\tilde{\Phi}$ is a solution of the linear problem

$$\begin{cases} -\epsilon_p \Delta \tilde{\Phi}(\mathbf{r}) = 0, & \mathbf{r} \in D_p, \\ -\nabla \cdot \left(\epsilon_\infty \nabla \tilde{\Phi}(\mathbf{r}) + (\epsilon_s - \epsilon_\infty) \nabla (Q_\lambda * \tilde{\Phi})(\mathbf{r})\right) \\ \qquad - \dfrac{e_c^2}{\epsilon_0 k_B T} B_1(\mathbf{r}) \tilde{\Phi}(\mathbf{r}) = \dfrac{e_c^2}{\epsilon_0 k_B T} A_1(\mathbf{r}), & \mathbf{r} \in D_s, \end{cases} \tag{4.2.13}$$

subject to the interface conditions

$$\tilde{\Phi}(\mathbf{s}^-) = \tilde{\Phi}(\mathbf{s}^+), \qquad \mathbf{s} \in \Gamma,$$
$$\epsilon_p \frac{\partial \tilde{\Phi}(\mathbf{s}^-)}{\partial \mathbf{n}(\mathbf{s})} = \epsilon_\infty \frac{\partial \tilde{\Phi}(\mathbf{s}^+)}{\partial \mathbf{n}(\mathbf{s})} + (\epsilon_s - \epsilon_\infty) \frac{\partial (\tilde{\Phi} * Q_\lambda)(\mathbf{s}^+)}{\partial \mathbf{n}(\mathbf{s})}, \quad \mathbf{s} \in \Gamma,$$

(4.2.14)

and the boundary conditions

$$\tilde{\Phi}(\mathbf{r}) \to 0 \qquad \text{as} \quad |\mathbf{r}| \to \infty.$$

(4.2.15)

In the above new linear model, to ensure the linearization would not introduce significant disturbance to the original nonlinear equation, the magnitude $|\tilde{\Phi}|$ needs to be sufficiently close to zero in the solvent domain D_s everywhere. Unfortunately, this condition may still not be satisfied in most real applications when the ionic strength is not weak enough. On the other hand, Proposition 4.2.1 reveals a fundamental principle: A linearization can only apply to a (component of a) function whose magnitude is close enough to zero. To improve Scheme A, we propose another linearization scheme as follows.

Proposition 4.2.3. *Suppose G and Ψ are pre-calculated. If there exists a given function W such that $|\tilde{\Phi}(\mathbf{r}) - W(\mathbf{r})|$ is sufficiently close to zero, then the Boltzmann term can be linearized by*

$$\sum_{i=1}^{n} Z_i M_i e^{-Z_i \Phi(\mathbf{r})}$$
$$\approx A_2(\mathbf{r}) - B_2(\mathbf{r}) \tilde{\Phi}(\mathbf{r})$$

(4.2.16)

where

$$A_2(\mathbf{r}) = \sum_{i=1}^{n} \left(1 + Z_i W(\mathbf{r})\right) Z_i M_i e^{-Z_i [G(\mathbf{r}) + \Psi(\mathbf{r}) + W(\mathbf{r})]},$$

(4.2.17)

and

$$B_2(\mathbf{r}) = \sum_{i=1}^{n} -Z_i^2 M_i e^{-Z_i [G(\mathbf{r}) + \Psi(\mathbf{r}) + W(\mathbf{r})]}.$$

(4.2.18)

Proof. The proof is similar as the one of Proposition 4.2.1, the linearization was applied at

the third step in the following derivations

$$\sum_{i=1}^{n} Z_i M_i e^{-Z_i \Phi(\mathbf{r})}$$

$$= \sum_{i=1}^{n} Z_i M_i e^{-Z_i[G(\mathbf{r}) + \Psi(\mathbf{r}) + W(\mathbf{r}) - W(\mathbf{r}) + \tilde{\Phi}(\mathbf{r})]}$$

$$= \sum_{i=1}^{n} Z_i M_i e^{-Z_i[G(\mathbf{r}) + \Psi(\mathbf{r}) + W(\mathbf{r})]} e^{-Z_i(\tilde{\Phi}(\mathbf{r}) - W(\mathbf{r}))}$$

$$\approx \sum_{i=1}^{n} Z_i M_i e^{-Z_i[G(\mathbf{r}) + \Psi(\mathbf{r}) + W(\mathbf{r})]} \left(1 - Z_i(\tilde{\Phi}(\mathbf{r}) - W(\mathbf{r}))\right) \qquad (4.2.19)$$

$$= \sum_{i=1}^{n} \left(\left(1 + Z_i W(\mathbf{r})\right) Z_i M_i e^{-Z_i[G(\mathbf{r}) + \Psi(\mathbf{r}) + W(\mathbf{r})]} \right.$$

$$\left. - Z_i^2 M_i e^{-Z_i[G(\mathbf{r}) + \Psi(\mathbf{r}) + W(\mathbf{r})]} \tilde{\Phi}(\mathbf{r}) \right)$$

$$= A_2(\mathbf{r}) + B_2(\mathbf{r})\tilde{\Phi}(\mathbf{r}) \qquad \forall \mathbf{r} \in D_s.$$

$\square$

Remark 4.2.4. For the 1:1 ionic solution, the linearization can be performed as

$$\sinh(\Phi(\mathbf{r}))$$
$$= \sinh(G(\mathbf{r}) + \Psi(\mathbf{r}) + W(\mathbf{r}) - W(\mathbf{r}) + \tilde{\Phi}(\mathbf{r}))$$
$$= \sinh((G(\mathbf{r}) + \Psi(\mathbf{r}) + W(\mathbf{r})) + (\tilde{\Phi}(\mathbf{r}) - W(\mathbf{r})))$$
$$\approx \sinh(G(\mathbf{r}) + \Psi(\mathbf{r}) + W(\mathbf{r})) + \cosh(G(\mathbf{r}) + \Psi(\mathbf{r}) + W(\mathbf{r}))(\tilde{\Phi}(\mathbf{r}) - W(\mathbf{r})) \qquad (4.2.20)$$
$$= \sinh(G(\mathbf{r}) + \Psi(\mathbf{r}) + W(\mathbf{r})) - \cosh(G(\mathbf{r}) + \Psi(\mathbf{r}) + W(\mathbf{r}))W(\mathbf{r})$$
$$\quad + \cosh(G(\mathbf{r}) + \Psi(\mathbf{r}) + W(\mathbf{r}))\tilde{\Phi}(\mathbf{r}), \qquad \forall \mathbf{r} \in D_s.$$

According to Proposition 4.2.3, we get the following linear equation for solving $\tilde{\Phi}$:

$$\begin{cases} -\epsilon_p \Delta \tilde{\Phi}(\mathbf{r}) = 0, & \mathbf{r} \in D_p, \\ -\nabla \cdot \left(\epsilon_\infty \nabla \tilde{\Phi}(\mathbf{r}) + (\epsilon_s - \epsilon_\infty)\nabla(Q_\lambda * \tilde{\Phi})(\mathbf{r}) \right) & \\ \quad -\dfrac{e_c^2}{\epsilon_0 k_B T} B_2(\mathbf{r})\tilde{\Phi}(\mathbf{r}) = A_2(\mathbf{r}), & \mathbf{r} \in D_s, \end{cases} \qquad (4.2.21)$$

with the same interface conditions (4.2.14) and boundary conditions (4.2.15) as in Proposition 4.2.1.

Remark 4.2.5. To ensure that Proposition 4.2.3 would work, a pre-determined function W is needed, which is expected to be an good approximation to $\tilde{\Phi}$ in the solvent domain. Although this looks an extravagant demand at the first glance, this scheme may still be valuable in many biomolecular dielectric application problems, in which cases a good approximation W may be constructed by some other simpler model results or from experimental data.

The above arguments provide an outline to solve the linearized nonlocal PBEs by new linearization schemes, we conclude it as the following algorithm.

Algorithm 4.2.6. *Solve linearized nonlocal PBE by new linearization schemes*

1. *Calculate G by (4.1.12).*

2. *Solve Ψ by (4.1.13), where G is used as a known function.*

3. *Solve $\tilde{\Phi}$ by (4.2.13) or by (4.2.21), where G and Ψ are used as two known functions.*

4. *Obtain $\Phi = G + \Psi + \tilde{\Phi}$.*

4.3 Numerical algorithms

In this section, we propose a numerical algorithm to solve the new linear nonlocal PBE by using the finite element method, and discuss some technique details in developing a program software package. Traditionally, the Poisson-Boltzmann equation is usually solved by using the finite difference method or its variants, due to its high efficiency. Two main reasons for us to choose the finite element method here are

1. The nonlocal PBE and its linearizations have strong singularities induced by the point charge terms. In Mathematics, these equations are only well-defined in their variational forms, and the finite element method is naturally designed to solve variational problems.

2. In many application problems involving PBE and nonlocal PBE, the object is one or multiple biomolecules with very a complicated three-dimensional geometrical shape. The classic finite different method usually ignores the interface condition defined on the biomolecular surface, which may introduce a significant error. On the other hand,

the finite element method does not have this difficulty. Because all interface conditions can be naturally included if the finite element space is chosen appropriately.

4.3.1 Reformulation into PDE systems

First, notice that if we program directly according to Algorithm (4.2.6) by the standard finite element method, the convolution terms $Q_\lambda * \Psi$ and $Q_\lambda * \tilde{\Phi}$ would induce dense stiffness matrices. This may make the programming implementation very hard and increase the computation cost drastically. Therefore, similar as solving the nonlocal Debye-Hückel equation in Chapter 3, we apply the reformulation technique to reformulate these integral-differential equations into pure PDE systems, such that the convolution terms can be removed. In particular, we regard the convolutions of G, Ψ, and $\tilde{\Phi}$ with kernel function Q_λ as three auxiliary functions, respectively. For the convolution of G, its analytical formula can be found, while for the other two, two equations can be built and coupled with (4.1.13) and (4.2.13) (or (4.2.21)) to form two systems of pure partial differential equations. In fact, we have the following algorithm.

Algorithm 4.3.1. *Denoting $u_0 = Q_\lambda * G$, $u_1 = Q_\lambda * \Psi$, and $u_2 = Q_\lambda * \tilde{\Phi}$, the solution Φ of the new linear nonlocal PBE (4.1.9) according to Proposition 4.2.1 can be obtained by:*

1. *Calculate G by*

$$G(\mathbf{r}) = \frac{e_c^2}{4\pi\epsilon_0\epsilon_p k_B T} \sum_{j=1}^{n_p} \frac{z_j}{|\mathbf{r} - \mathbf{r}_j|}, \tag{4.3.1}$$

and u_0 by

$$u_0(\mathbf{r}) = \frac{e_c^2}{4\pi\epsilon_0\epsilon_p k_B T} \sum_{j=1}^{n_p} \frac{z_j(1 - e^{-|\mathbf{r}|/\lambda})}{|\mathbf{r}|}. \tag{4.3.2}$$

2. *Solve Ψ and u_1 from the following system*

$$\begin{cases} \Delta\Psi(\mathbf{r}) = 0, & \mathbf{r} \in D_p, \\ -\epsilon_\infty\Delta\Psi(\mathbf{r}) + \frac{\epsilon_s - \epsilon_\infty}{\lambda^2}\Big(\Psi(\mathbf{r}) - u_1(\mathbf{r})\Big) = \frac{\epsilon_\infty - \epsilon_s}{\lambda^2}\Big(G(\mathbf{r}) - u_0(\mathbf{r})\Big), & \mathbf{r} \in D_s, \\ -\lambda^2\Delta u_1(\mathbf{r}) + u_1(\mathbf{r}) - \Psi(\mathbf{r}) = 0, & \mathbf{r} \in \mathbb{R}^3, \end{cases} \tag{4.3.3}$$

with boundary conditions

$$u_1(\mathbf{r}) \to 0, \quad \Psi(\mathbf{r}) \to 0 \qquad \text{as} \quad |\mathbf{r}| \to \infty, \tag{4.3.4}$$

46

and interface conditions

$$
\begin{cases}
\Psi(\mathbf{s}^-) = \Psi(\mathbf{s}^+), & \mathbf{s} \in \Gamma, \\
\epsilon_p \dfrac{\partial \Psi(\mathbf{s}^-)}{\partial \mathbf{n}(\mathbf{s})} = \epsilon_\infty \dfrac{\partial \Psi(\mathbf{s}^+)}{\partial \mathbf{n}(\mathbf{s})} + (\epsilon_s - \epsilon_\infty) \dfrac{\partial u_1(\mathbf{s})}{\partial \mathbf{n}(\mathbf{s})} \\
\quad + (\epsilon_s - \epsilon_\infty) \dfrac{\partial u_0(\mathbf{s})}{\partial \mathbf{n}(\mathbf{s})} + (\epsilon_\infty - \epsilon_p) \dfrac{\partial G(\mathbf{s})}{\partial \mathbf{n}(\mathbf{s})}, & \mathbf{s} \in \Gamma.
\end{cases}
\tag{4.3.5}
$$

3. *Solve $\tilde{\Phi}$ and u_2 from the following system*

$$
\begin{cases}
\Delta \tilde{\Phi}(\mathbf{r}) = 0, & \mathbf{r} \in D_p, \\
-\epsilon_\infty \Delta \tilde{\Phi}(\mathbf{r}) + \dfrac{\epsilon_s - \epsilon_\infty}{\lambda^2}\left(\tilde{\Phi}(\mathbf{r}) - u_2(\mathbf{r}) \right) \\
\quad + \dfrac{e_c^2}{\epsilon_0 k_B T} Z_i^2 M_i e^{-Z_i[G(\mathbf{r})+\Psi(\mathbf{r})]} \tilde{\Phi}(\mathbf{r}) = \displaystyle\sum_{i=1}^n Z_i M_i e^{-Z_i[G(\mathbf{r})+\Psi(\mathbf{r})]}, & \mathbf{r} \in D_s, \\
-\lambda^2 \Delta u_2(\mathbf{r}) + u_2(\mathbf{r}) - \tilde{\Phi}(\mathbf{r}) = 0, & \mathbf{r} \in \mathbb{R}^3,
\end{cases}
\tag{4.3.6}
$$

with boundary conditions

$$
u_2(\mathbf{r}) \to 0, \quad \tilde{\Phi}(\mathbf{r}) \to 0 \qquad \text{as} \quad |\mathbf{r}| \to \infty,
\tag{4.3.7}
$$

and interface conditions

$$
\begin{cases}
\tilde{\Phi}(\mathbf{s}^-) = \tilde{\Phi}(\mathbf{s}^+), & \mathbf{s} \in \Gamma, \\
\epsilon_p \dfrac{\partial \tilde{\Phi}(\mathbf{s}^-)}{\partial \mathbf{n}(\mathbf{s})} = \epsilon_\infty \dfrac{\partial \tilde{\Phi}(\mathbf{s}^+)}{\partial \mathbf{n}(\mathbf{s})} + (\epsilon_s - \epsilon_\infty) \dfrac{\partial u_2(\mathbf{s})}{\partial \mathbf{n}(\mathbf{s})}, & \mathbf{s} \in \Gamma.
\end{cases}
\tag{4.3.8}
$$

4. *Obtain the solution by*

$$
\Phi(\mathbf{r}) = \tilde{\Phi}(\mathbf{r}) + \Psi(\mathbf{r}) + G(\mathbf{r}).
\tag{4.3.9}
$$

The solution of (4.2.21) according to Proposition 4.2.3 can be obtained by the same procedure, only except for replacing (4.3.6) by the following equation when for solving $\tilde{\Phi}$:

$$
\begin{cases}
\Delta \tilde{\Phi}(\mathbf{r}) = 0, & \mathbf{r} \in D_p, \\
-\nabla \cdot \left(\epsilon_\infty \nabla \tilde{\Phi}(\mathbf{r}) + (\epsilon_s - \epsilon_\infty) \nabla u_2(\mathbf{r}) \right) + \dfrac{e_c^2}{\epsilon_0 k_B T} \displaystyle\sum_{i=1}^n Z_i^2 M_i e^{-Z_i[G(\mathbf{r})+\Psi(\mathbf{r})+W(\mathbf{r})]} \tilde{\Phi}(\mathbf{r}) \\
\quad = \displaystyle\sum_{i=1}^n (1 + Z_i W(\mathbf{r})) M_i e^{-Z_i[G(\mathbf{r})+\Psi(\mathbf{r})+W(\mathbf{r})]}, & \mathbf{r} \in D_s, \\
-\lambda^2 \Delta u_2(\mathbf{r}) + u_2(\mathbf{r}) - \tilde{\Phi}(\mathbf{r}) = 0, & \mathbf{r} \in \mathbb{R}^3,
\end{cases}
\tag{4.3.10}
$$

where W is a pre-determined function that is expected to be a good approximation of $\tilde{\Phi}$ in the solvent domain D_s.

4.3.2 Variational forms

Here, we restrict our discussion to a bounded domain Ω which is large enough to hold D_p, such that

$$\Omega = D_p \cup D_s \cup \Gamma.$$

The variational form of a partial differential equation can be obtained by multiplying a test function on both sides the equation, then taking integrals on Ω and applying Green's identities. We denote U and V as trial function spaces defined on Ω, and $U_0 = \{u | u \in U, u|_{\partial\Omega} = 0\}$, $V_0 = \{v | v \in V, v|_{\partial\Omega} = 0\}$ as the test function spaces.

Proposition 4.3.2. (The variational problem for solving Ψ) *Provided G and u_0 defined by (4.3.1) and (4.3.2) respectively, find (Ψ, u_1) in the product space $U \times V$, such that*

$$\epsilon_p \int_{D_p} \nabla\Psi(\mathbf{r}) \cdot \nabla v_1(\mathbf{r}) d\mathbf{r} + \epsilon_\infty \int_{D_s} \nabla\Psi(\mathbf{r}) \cdot \nabla v_1(\mathbf{r}) d\mathbf{r} + (\epsilon_s - \epsilon_\infty) \int_{D_s} \nabla u_1(\mathbf{r}) \cdot \nabla v_1(\mathbf{r}) d\mathbf{r}$$

$$+ \lambda^2 \int_\Omega \nabla u_1(\mathbf{r}) \cdot \nabla v_2(\mathbf{r}) d\mathbf{r} + \int_\Omega \Big(u_1(\mathbf{r}) - \Psi(\mathbf{r}) \Big) v_2(\mathbf{r}) d\mathbf{r}$$

$$= (\epsilon_\infty - \epsilon_s) \int_{D_s} \nabla u_0(\mathbf{r}) \cdot \nabla v_1(\mathbf{r}) d\mathbf{r} + (\epsilon_p - \epsilon_\infty) \int_{D_s} \nabla G(\mathbf{r}) \cdot \nabla v_1(\mathbf{r}) d\mathbf{r},$$

(4.3.11)

for any $v_1 \in U_0$ and any $v_2 \in V_0$.

Proposition 4.3.3. (The variational problems for solving $\tilde{\Phi}$ by Proposition 4.2.1) *Provided G and u_0 defined by (4.3.1) and (4.3.2) respectively, and suppose Ψ has been solved previously from (4.3.11). Find $(\tilde{\Phi}, u_2)$ in $U \times V$, such that*

$$\epsilon_p \int_{D_p} \nabla\tilde{\Phi}(\mathbf{r}) \cdot \nabla v_1(\mathbf{r}) d\mathbf{r} + \epsilon_\infty \int_{D_s} \nabla\tilde{\Phi}(\mathbf{r}) \cdot \nabla v_{(\mathbf{r})} d\mathbf{r}$$

$$+ (\epsilon_s - \epsilon_\infty) \int_{D_s} \nabla u_2(\mathbf{r}) \cdot \nabla v_1(\mathbf{r}) d\mathbf{r} + \frac{e_c^2}{\epsilon_0 k_B T} \sum_{i=1}^n Z_i^2 M_i \int_{D_s} e^{-Z_i[G(\mathbf{r})+\Psi(\mathbf{r})]} \tilde{\Phi}(\mathbf{r}) v_1(\mathbf{r}) d\mathbf{r}$$

(4.3.12)

$$+ \lambda^2 \int_\Omega \nabla u_2(\mathbf{r}) \cdot \nabla v_2(\mathbf{r}) d\mathbf{r} + \int_\Omega \Big(u_2(\mathbf{r}) - \tilde{\Phi}(\mathbf{r}) \Big) v_2(\mathbf{r}) d\mathbf{r}$$

$$= \sum_{i=1}^n Z_i M_i \int_{D_s} e^{-Z_i[G(\mathbf{r})+\Psi(\mathbf{r})]} v_1(\mathbf{r}) d\mathbf{r}$$

for any $v_1 \in U_0$ and any $v_2 \in V_0$.

Proposition 4.3.4. (The variational problems for solving $\tilde{\Phi}$ by Proposition 4.2.3) *Provided G and u_0 defined by* (4.3.1) *and* (4.3.2) *respectively, and suppose Ψ has been solved previously from variational problem* (4.3.11). *Find* $(\tilde{\Phi}, u_2)$ *in $U \times V$, such that*

$$
\epsilon_p \int_{D_p} \nabla \tilde{\Phi}(\mathbf{r}) \cdot \nabla v_1(\mathbf{r}) \mathrm{d}\mathbf{r} + \epsilon_\infty \int_{D_s} \nabla \tilde{\Phi}(\mathbf{r}) \cdot \nabla v_(\mathbf{r}) \mathrm{d}\mathbf{r}
$$

$$
+ (\epsilon_s - \epsilon_\infty) \int_{D_s} \nabla u_2(\mathbf{r}) \cdot \nabla v_1(\mathbf{r}) \mathrm{d}\mathbf{r} + \frac{e_c^2}{\epsilon_0 k_B T} \sum_{i=1}^n Z_i^2 M_i \int_{D_s} e^{-Z_i[G(\mathbf{r}) + \Psi(\mathbf{r}) + W(\mathbf{r})]} \tilde{\Phi}(\mathbf{r}) v_1(\mathbf{r}) \mathrm{d}\mathbf{r}
$$

$$
+ \lambda^2 \int_\Omega \nabla u_2(\mathbf{r}) \cdot \nabla v_2(\mathbf{r}) \mathrm{d}\mathbf{r} + \int_\Omega \left(u_2(\mathbf{r}) - \tilde{\Phi}(\mathbf{r}) \right) v_2(\mathbf{r}) \mathrm{d}\mathbf{r}
$$

$$
= \sum_{i=1}^n Z_i M_i \int_{D_s} e^{-Z_i[G(\mathbf{r}) + \Psi(\mathbf{r})]} v_1(\mathbf{r}) \mathrm{d}\mathbf{r}
$$

$$(4.3.13)$$

for any $v_1 \in U_0$ and any $v_2 \in V_0$.

Chapter 5

Program Package and Numerical Results

Software is the realization of numerical theory and algorithm. As an implementation of our nonlocal Debye-Hückel equations and nonlocal Poisson-Boltzmann equations, we developed a software program package to solve these equations. We validated this program package on some model problems whose analytical solutions are viable. We then use it to solve some simple applications, which exhibits its potential to be valuable in more practical problems. All these tests were completed on a Mac Pro workstation with one 3.7 GHz Intel Xeon E5 processor and 64 GB memory.

5.1   Software program package development

According to the numerical algorithms described in Chapter 3 and Chapter 4, we developed a finite element program package to solve the nonlocal Debye-Hückel equations and the new linear nonlocal Poisson-Boltzmann equations. This package is programmed in a combination of Python, C/C++ and Fortran programming languages. Particularly, it is built based on the popular finite element library `DOLFIN` from the FEniCS project [77, 78], which contains many finite element bases, fast linear solvers and useful technical tools. It provides a platform for programming PDE variational problems in a concise way, in the mean time, keeps high efficiency on underlying numerical calculations. To solve biomolecular cases, we created a mesh generator based on two three-dimensional mesh structure packages: `GAMer` [79] and `Tetgen` [80]. This mesh generator can be easily used, as users only need to prepare a

protein data bank (PDB) file for a protein structure [81, 82], and input several mesh control parameters. The generator will automatically identify the protein surface, either according to an analytic expression or by using a probe rolling ball, and then generate a triangular mesh that preserves the geometry of the protein surface. This surface mesh will be passed to `Tetgen` for filling in cells to create a complete tetrahedral mesh that can be used in finite element calculations. The whole mesh generation process has been observed being very efficient and robust when appropriate mesh parameters are chosen. Besides, we programmed several Fortran subroutines for efficiently calculating G, ∇G and their convolutions according to analytical formulas. At last, we wrote all main driver files in Python scripts to provide a user-friendly interface of our package on the top level. All other language packages have been converted into Python modules by using `SWIG` [83] (for C/C++) or `F2PY` [84] (for Fortran) such that they can be easily invoked in the driver files.

5.2 Validations on the nonlocal Debye-Hückel equation

5.2.1 A center point charge case

We first test the nonlocal Debye-Hückel equation (3.4.1) for one single charge locateing at the origin, i.e., $n_p = 1, z_1 = z$. In this case, (3.4.1) reduces to

$$
\begin{cases}
-\epsilon_\infty \Delta \Phi(\mathbf{r}) + (\epsilon_s - \epsilon_\infty) \nabla \cdot \int_{\mathbb{R}^3} Q_\lambda(\mathbf{r} - \mathbf{r}') \nabla \Phi(\mathbf{r}') \mathrm{d}\mathbf{r}' \\
\qquad\qquad + \dfrac{2Me^2}{\epsilon_0 k_B T} \Phi(\mathbf{r}) = \dfrac{e_c^2 z \delta}{\epsilon_0 k_B T}, & \mathbf{r} \in \Omega, \\
\qquad\qquad\qquad \Phi(\mathbf{s}) = 0, & \mathbf{s} \in \partial\Omega.
\end{cases} \tag{5.2.1}
$$

Using the solution decomposition and reformulation techniques, we will solve Ψ and u_1 as the solution of (3.4.6) with G and u_0 defined by

$$
G(\mathbf{r}) = \frac{e_c^2 z}{4\pi\epsilon_0 \epsilon_p k_B T} \qquad \text{and} \qquad u_0(\mathbf{r}) = \frac{e_c^2 z}{4\pi\epsilon_0 \epsilon_p k_B T}. \tag{5.2.2}
$$

Denote Ψ and u_1 as the analytic solutions and Ψ_h and $u_{1,h}$ as numerical solution. We define the relative error by

$$
\frac{\|\Psi - \Psi_h\|}{\|\Psi\|} = \sqrt{\frac{\int_\Omega |\Psi(\mathbf{r}) - \Psi_h(\mathbf{r})|^2 \mathrm{d}\mathbf{r}}{\int_\Omega |\Psi(\mathbf{r})|^2 \mathrm{d}\mathbf{r}}}, \tag{5.2.3}
$$

51

and an average relative error, $E_{rel}(v)$ by

$$E_{rel}(v) = \frac{1}{N}\sqrt{\sum_{j=1}^{N}\left(\frac{v(\mathbf{r}^j) - v_h(\mathbf{r}^j)}{v(\mathbf{r}^j)}\right)^2}, \qquad (5.2.4)$$

where v_h denotes a finite element approximation to v on a mesh with N nodes (degrees of freedom) and $\mathbf{r}^j$ being the jth node.

In the test, we set domain $\Omega = \{\mathbf{r}|\|\mathbf{r}\| < 10[\text{Å}]\}$, $z = 1, \epsilon_\infty = 1.8, \epsilon_s = 78.54, T = 298.15[\text{K}]$, $\lambda = 15[\text{Å}]$, and $I_s = 0.1[\text{mol/L}]$. A tetrahedral mesh of Ω used in this test has 2,955 vertices. A cross-section view of the mesh is shown in Figure 5.1:
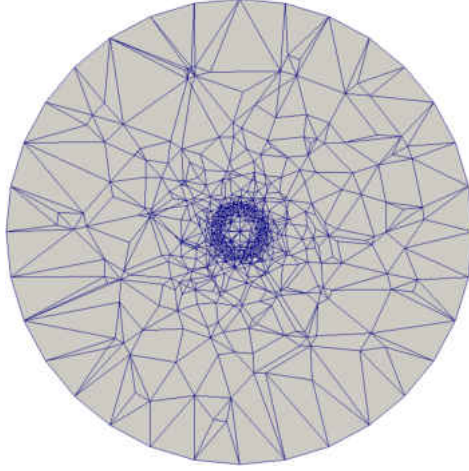
Figure 5.1: A cross-section view of the tetrahedral mesh used in the validation test for one charge case.

We repeat the tests for the finite element product space $U_h \times V_h$, with U_h and V_h being the linear, quadratic, and cubic Lagrangian polynomial function spaces, respectively. The errors of numerical solutions for each case are reported in Table 5.1.

5.2.2 Multiple charges

We also test this model for the case of multiple charges that are extracted from real protein atomic structures. To avoid the singularity induced by Green's function G as the right hand side of (3.4.6) in the assembling process, we use meshes only defining on an exterior domain Ω which excluding all protein atoms, thus there are one interior and one exterior boundary

$U_h \times V_h$ order	Degree of freedoms	$\frac{\|\Psi - \Psi_h\|}{\|\Psi\|}$	$\frac{\|u_1 - u_{1,h}\|}{\|u_1\|}$	$E_{rel}(\Psi)$	$E_{rel}(u_1)$
$(1, 1)$	2955×2	6.83E−1	2.37E−2	3.86E−2	2.06E−3
$(2, 2)$	23522×2	1.37E−1	5.71E−3	2.94E−3	1.75E−4
$(3, 3)$	79059×2	6.73E−2	2.79E−3	7.85E−4	4.66E−5

Table 5.1: Numeric errors of Ψ and u_1 by using linear, quadratic and cubic finite element function spaces for one central charge.

of Ω, both of which are applied the true solution boundary conditions in the calculation. All the model parameters and constants are set the same as the previous case.

We tested three sets of charges from three protein molecules with PDB ID: 2LZX, 1UCS, and 1AQ5 respectively, Box-Clip views of the meshes used for the tests are shown in Figure 5.2.

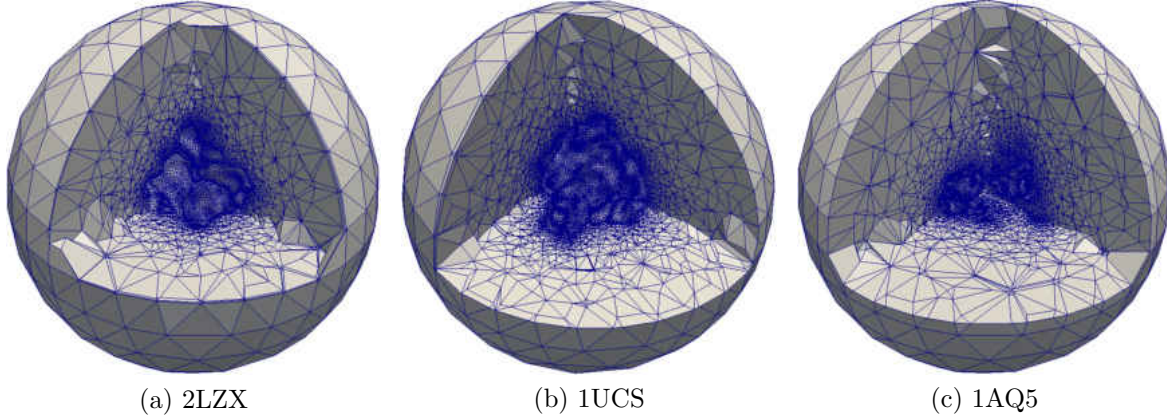(a) 2LZX   (b) 1UCS   (c) 1AQ5

Figure 5.2: Box-Clip views of the three tetrahedral meshes used for numerical validations for multiple charge cases.

Similar to the one-point charge case, we did tests using the linear, quadratic and cubic finite element methods. The relative error in the L_2 norm and the average relative error E_{rel}. The test results are collected in Table 5.2:

PDB (#atoms)	$U_h \times V_h$ order	Degree of freedoms	$\frac{\|\Psi - \Psi_h\|_{L_2}}{\|\Psi\|_{L_2}}$	$\frac{\|u_1 - u_{1,h}\|_{L_2}}{\|u_1\|_{L_2}}$	$E_{rel}(\Psi)$	$E_{rel}(u_1)$
2LZX	$(1,1)$	33658×2	1.50E−3	1.49E−3	5.86E−6	4.57E−6
(488)	$(2,2)$	180271×2	1.58E−4	6.55E−5	1.67E−7	3.37E−8
	$(3,3)$	819626×2	1.83E−5	6.19E−6	8.54E−9	1.26E−9
1UCS	$(1,1)$	48648×2	6.23E−3	1.38E−2	1.86E−2	2.06E−3
(997)	$(2,2)$	360542×2	7.89E−4	6.74E−4	1.10E−4	6.42E−4
	$(3,3)$	1179153×2	1.04E−4	6.95E−5	6.22E−6	1.44E−5
1AQ5	$(1,1)$	47557×2	2.14E−3	3.01E−3	2.26E−3	6.03E−6
(2292)	$(2,2)$	355628×2	2.59E−4	1.96E−4	2.05E−4	8.11E−8
	$(3,3)$	1166522×2	3.59E−5	2.05E−5	1.70E−5	3.54E−9

Table 5.2: Numeric errors of finite element solutions Ψ_h and $u_{1,h}$ spaces for the three sets of charges from three proteins (PDB ID: 2LZX, 1UCS, and 1AQ5), respectively.

5.3 Solving new linear nonlocal Poisson-Boltzmann equations

5.3.1 A nonlocal Born model

To verify our finite element program for solving the new linearized nonlocal Poisson-Boltzmann equation, we first consider a model problem whose analytical solution is available. Suppose D_p is a ball centering at the origin with radius a, which represents the solute domain. At the origin, there is one single point charge with charge quantity z. Thus, under these settings, we get a specific case of the nonlocal Poisson equation (2.4.11) for $\rho = z\delta$. For clarity, we write this model in (5.3.1) and call it the nonlocal Born ball model. Note that it has been reformulated in a system of PDEs.

$$
\begin{cases}
-\epsilon_p \Delta \Phi(\mathbf{r}) = \alpha z \delta, & |\mathbf{r}| < a, \\
-\epsilon_\infty \Delta \Phi(\mathbf{r}) + \alpha_1\Big(\Phi(\mathbf{r}) - (\Phi * Q_\lambda)(\mathbf{r})\Big) = 0, & |\mathbf{r}| > a, \\
\Phi(\mathbf{s}^-) = \Phi(\mathbf{s}^+), & |\mathbf{s}| = a, \\
\epsilon_p \frac{\partial \Phi(\mathbf{s}^-)}{\partial \mathbf{n}(\mathbf{s})} = \epsilon_\infty \frac{\partial \Phi(\mathbf{s}^+)}{\partial \mathbf{n}(\mathbf{s})} + (\epsilon_s - \epsilon_\infty)\frac{\partial (\Phi * Q_\lambda)(\mathbf{s})}{\partial \mathbf{n}(\mathbf{s})}, & |\mathbf{s}| = a, \\
\Phi(\mathbf{r}) \to 0 & \text{as} \quad |\mathbf{r}| \to \infty.
\end{cases}
\tag{5.3.1}
$$

It has been proved that the solution of the above equation has the following analytical form [85]:

$$\Phi(\mathbf{r}) = \begin{cases} \dfrac{\alpha z}{4\pi a \epsilon_p \epsilon_s} \left(\dfrac{a\epsilon_s}{|\mathbf{r}|} + \epsilon_p - \epsilon_s - (\epsilon_\infty - \epsilon_s) b_1 \right) & \mathbf{r} \in D_p, \\ \dfrac{\alpha z}{4\pi \epsilon_p \epsilon_s |\mathbf{r}|} \left(\epsilon_p - (\epsilon_\infty - \epsilon_s) b_1 e^{\mu(a - |\mathbf{r}|)} \right) & \mathbf{r} \in D_s, \end{cases} \tag{5.3.2}$$

where the constants $b_1, b_2,$ and μ are defined as

$$\mu = \frac{1}{\lambda} \sqrt{\frac{\epsilon_s}{\epsilon_\infty}}, \tag{5.3.3}$$

$$b_1 = \frac{a\epsilon_s + \lambda(\epsilon_p - \epsilon_s) \sinh \frac{a}{\lambda}}{[a\sqrt{\epsilon_\infty \epsilon_s} + \lambda \sinh \frac{a}{\lambda}] + a\epsilon_s \cosh \frac{a}{\lambda}}, \tag{5.3.4}$$

and

$$b_2 = \frac{[a\sqrt{\epsilon_\infty \epsilon_s} + \lambda(\epsilon_\infty - \epsilon_s) - a\epsilon_s] e^{-\frac{a}{\lambda}} + \lambda(\epsilon_s - \epsilon_p)}{[a\sqrt{\epsilon_\infty \epsilon_s} + \lambda(\epsilon_\infty - \epsilon_s)] \sinh \frac{a}{\lambda} + a\epsilon_s \cosh \frac{a}{\lambda}}. \tag{5.3.5}$$

In the test, we use Ω as the unit ball centering at the origin, and set $a = 0.1, \epsilon_p = 2, \epsilon_s = 78.54,$ and $\lambda = 15,$ all other parameters are evaluate by their real physical values. Besides, We use the same mesh as the one used in Section 5.2.1. We also repeat the tests for $U_h \times V_h$ set as the product of the linear, quadratic, and cubic Lagrangian polynomial function spaces, respectively. For each case, we report the absolute and relative L_2 errors of numerical solutions for each case are reported in Table 5.3. Here, the absolute error of a numerical solution Φ_h for the true solution Φ is defined as

$$\|\Phi_h - \Phi\| = \int_\Omega \left[\Phi_h(\mathbf{r}) - \Phi(\mathbf{r}) \right]^2 d\mathbf{r}, \tag{5.3.6}$$

and the relative error is defined as $\|\Phi_h - \Phi\| / \|\Phi\|$.

The numerical results shows that as the finite element order raises from 1 to 3, the relative error of the numerical solution reduces from the order of 10^{-4} to 10^{-6}. It validates that our finite element software is accurate.

5.3.2 Proteins in electrolytes

Here, we solve the new linear nonlocal PBE (by Proposition 4.2.1) for a series of proteins (identified by their PDB IDs) immerse in ionic solution. For each case, the calculating domain Ω is set as a ball with the protein locating at its center. The radius of Ω is three times large as the one of the circumsphere of protein. In the test, the ionic solution contains

FEM	Error	
Order k	$\|\Phi - \Phi_h\|$	$\|\Phi - \Phi_h\|/\|\Phi\|$
1	5.849E−4	4.611E−3
2	4.760E−5	3.752E−4
3	8.250E−6	6.503E−5

Table 5.3: Errors of the numerical solutions of the nonlocal Born model (5.3.1) by using our finite element software package. The equation is solved in the linear, quadratic and cubic Lagrangian finite element space, with 2955, 23522 and 79059 unknowns, respectively.

two monovalent ions carrying opposite charges (e.g. NaCl), with the ionic strength set as 0.1 mol/L, the nonlocal correlation length λ is set to be 15 Å, all other parameters are set as their real physical values as shown in Table 2.1 and Table 2.2. We collected the central processor unit (CPU) times for each step in the solution process in Table 5.4.

As we can see from Table 5.4, Ψ and $\tilde{\Phi}$ can be solved very quickly by our finite element package, as they can be found in 10 seconds for most cases. On the other hand, mesh generation and/or calculating function G and its gradient are the two most time costly steps in the solution process. This test shows that our finite element package is very efficient, but also suggests the further improvement on mesh generations to reduce the total calculation cost.

We also compared the solutions of the local linearized PBE, the traditional linearized nonlocal PBE and the new linearized nonlocal PBE, respectively. We plotted the electrostatic potential on the surface of a protein in Figure 5.3, and on one cross-section plane of Ω in Figure 5.4, respectively. These figures are plotted by VMD [3], and ParaView [86], respectively. Color at each point is determined by the value of the electrostatic potential Φ, which is measured in the dimensionless form (i.e., under the unit $k_B T/e_c$). To get a better visualization experience, Φ's value were truncated to $-50 \sim 50$ (surface potential view) and $-5 \sim 5$ (cross section potential view) as the lower and upper bounds of the coloring scheme, respectively. In this comparison test, all experimental settings are the same as the previous one.

PDB ID	Protein atoms	Mesh vertices	CPU time (seconds) and percentage				
			Generate mesh	$G, \nabla G$, etc.	Solve Ψ	Solve$\tilde{\Phi}$	Total cpu time
2LZX	488	39658	12.6(52.8%)	2.5(10.5%)	3.1(13.0%)	2.8(11.8%)	21.1(100%)
1AJJ	513	55451	17.0(50.0%)	3.7(11.0%)	4.8(14.3%)	4.5(13.2%)	29.9(100%)
1FXD	811	58876	18.3(47.0%)	6.3(16.1%)	5.6(14.3%)	4.7(12.0%)	34.9(100%)
4PTI	892	67701	20.8(37.2%)	8.3(14.9%)	11.6(20.8%)	9.4(16.7%)	9.4(100%)
1CID	2783	32968	13.9(42.0%)	11.9(35.9%)	2.5(7.5%)	2.2(6.6%)	30.5(100%)
2AQ5	6024	62045	27.1(30.0%)	48.3(53.3%)	5.7(6.4%)	4.8(5.2%)	85.9(100%)
1HPT	852	22666	8.7(54.7%)	2.5(15.8%)	1.5(9.6%)	1.4(9.0%)	14.2(100%)
1SVR	1433	30654	11.4(47.7%)	5.7(24.0%)	2.3(9/6%)	2.0(8.5%)	21.3(100%)
1A63	2065	38287	16.0(46.0%)	10.3(29.5%)	3.1(8.8%)	2.6(7.5%)	32.0(100%)
1A7M	2803	34478	14.6(42.1%)	12.5(36.0%)	2.8(8.0%)	2.3(6.7%)	32.2(100%)
1F6W	8243	23923	21.6(41.6%)	25.6(49.2%)	1.7(3.2%)	1.4(2.7%)	50.2(100%)
1C4K	11439	32690	30.8(35.4%)	49.0(56.4%)	2.6(3.0%)	2.1(2.4%)	84.5(100%)

Table 5.4: CPU time for solving the new linear nonlocal PBE (Proposition 4.2.1) on twelve proteins that have number of atoms range from 513 to 11439. Here, we list the CPU time of each main step in the solution process and their percentages out of the total time. For most of cases, all calculations including mesh generation can be finished within one minute, this shows the high efficiency of our finite element package.

(a) Linearized PBE   (b) Traditional linearized   (c) New linearized nonlocal PBE
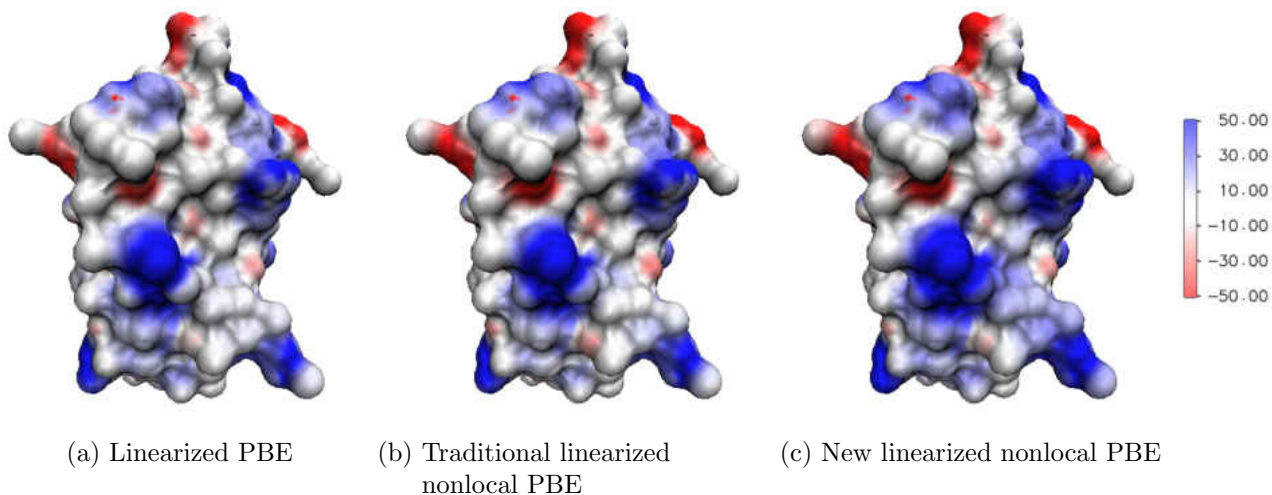   nonlocal PBE

Figure 5.3: Electrostatic potential distributions on the surface of a protein (PDB ID: 4PTI) as the solutions of linearized PBE, the traditional linearized nonlocal PBE, and the new linearized nonlocal PBE (Proposition 4.2.1), respectively. The figures are colored according to the value of Φ at each point on the protein surface. Φ's value were truncated at -50 and 50 as the lower and upper bounds of the coloring scheme, as the dimensionless value (i.e., under the unit $k_B T / e_c$). This figure is plotted by VMD.
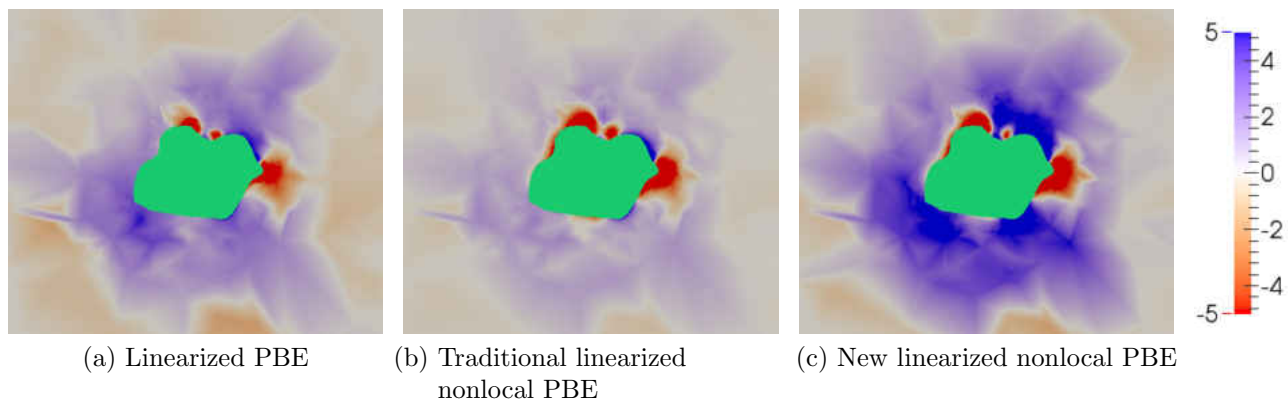

(a) Linearized PBE   (b) Traditional linearized   (c) New linearized nonlocal PBE
                        nonlocal PBE

Figure 5.4: A cross-section view of the electrostatic potential Φ in neighboring area around a protein (PDB ID: 4PTI) surface in an ionic solution. The pictures are colored according to the value of Φ at each point on the slice-cutting plane. In the coloring scheme, Φ's value were truncated at -5 and 5 as the lower and upper bounds (under the unit $k_B T / e_c$). The green domain in the center represents the protein area on this slice cut. This figure is plotted by ParaView.

Chapter 6

Conclusions

In this dissertation, a numerical method for investigating electrostatic dielectric properties of aqueous electrolytes was studied. This method is based on the continuum solvent approach, and combines the classic Poisson-Boltzmann theory and the nonlocal dielectric modeling scheme. In this way, a mathematical framework was built for nonlocal electrostatic models, which is described in an integral-differential equation with respect to the unknown function Φ, the electrostatic potential. As two specific cases, this framework was studied in two different contexts, one for a single solvent domain case and the other for multiple dielectric domain case, respectively. Correspondingly, two specific nonlocal dielectric models are proposed respectively: the Debye-Hückel equation and the nonlocal Poisson-Boltzmann equation. Both these two equations consider the nonlocal dielectric effect as a convolution term which describes the nonlocal response between the electric field and the displacement field. They also assume that the concentration functions of dissolved ions satisfy the nonlinear Boltzmann distributions. To analyze and solve these models, a reformulation scheme was applied to eliminate the convolution term, such that their are rewritten into a system of partial differential equations from the original integral-differential form. Besides, to overcome the difficulties induces by the Dirac delta singularity, a solution decomposition technique was used to split the original solution into two or three components such that one carries all singularities with explicit algebraic formula, and the others satisfy well defined equations. The nonlocal Debye-Hückel equations are suitable for a pure solution domain case, such as the electric double layer problems, which has a simpler mathematical form and easier to analyze. Particularly, in this thesis, a linearized nonlocal Debye-Hückel equation

was thoroughly studied and its analytical solution was found in algebraic form. This result may be very useful in setting the boundary values for solving nonlinear problems. On the other hand, the nonlocal Poisson-Boltzmann equations are more complicated due to multiple domains are involved. But this characteristics makes them especially valuable in applications involving multiple mediums, such as biomolecules immersed in electrolytes. In this thesis, we proposed a linearized nonlocal Poisson-Boltzmann by using a new linearization scheme. This new scheme was developed based on the solution decomposition technique as previously mentioned. It carefully chooses the component of the unknown function to be linearized, such that it is expected to induce less disturbance and achieve a better approximation to the original nonlinear equation than the traditional scheme. It also provides a good initial guess for solving the full nonlinear equation. As last, based on the theoretic analyses, numerical algorithms and a finite element software package were developed to solve these models numerically, as well as to validate the analytical solution. According to the data of numerical tests, this software package is effective and efficient in solving partial differential equations and finding solutions.

BIBLIOGRAPHY

[1] S. Nosé, A molecular dynamics method for simulations in the canonical ensemble, Molecular physics 52 (2) (1984) 255–268.

[2] J. Haile, Molecular dynamics simulation, Vol. 18, Wiley, New York, 1992.

[3] W. Humphrey, A. Dalke, K. Schulten, Vmd: visual molecular dynamics, Journal of molecular graphics 14 (1) (1996) 33–38.

[4] C. J. Cramer, D. G. Truhlar, Implicit solvation models: equilibria, structure, spectra, and dynamics, Chemical Reviews 99 (8) (1999) 2161–2200.

[5] B. Roux, T. Simonson, Implicit solvent models, Biophysical chemistry 78 (1) (1999) 1–20.

[6] P. Ferrara, J. Apostolakis, A. Caflisch, Evaluation of a fast implicit solvent model for molecular dynamics simulations, Proteins: Structure, Function, and Bioinformatics 46 (1) (2002) 24–33.

[7] R. Zhou, Free energy landscape of protein folding in water: explicit vs. implicit solvent, Proteins: Structure, Function, and Bioinformatics 53 (2) (2003) 148–161.

[8] N. Baker, Improving implicit solvent simulations: a poisson-centric view, Current opinion in structural biology 15 (2) (2005) 137–143.

[9] C. Tan, Y.-H. Tan, R. Luo, Implicit nonpolar solvent models, The Journal of Physical Chemistry B 111 (42) (2007) 12263–12274.

[10] J. Chen, C. L. Brooks, J. Khandogin, Recent advances in implicit solvent-based methods for biomolecular simulations, Current Opinion in Structural Biology 18 (2) (2008) 140–148.

[11] P. Labute, The generalized born/volume integral implicit solvent model: estimation of the free energy of hydration using london dispersion instead of atomic surface area, Journal of computational chemistry 29 (10) (2008) 1693–1698.

[12] R. Car, M. Parrinello, Unified approach for molecular dynamics and density-functional theory, Physical review letters 55 (22) (1985) 2471.

[13] D. Chklovskii, B. Shklovskii, L. Glazman, Electrostatics of edge channels, Physical Review B 46 (7) (1992) 4026.

[14] B. Honig, A. Nicholls, Classical electrostatics in biology and chemistry, Science 268 (5214) (1995) 1144.

[15] M. Perutz, Electrostatic effects in proteins, Science 201 (4362) (1978) 1187–1191.

[16] N. Baker, D. Sept, S. Joseph, M. Holst, J. McCammon, Electrostatics of nanosystems: application to microtubules and the ribosome, Proceedings of the National Academy of Sciences 98 (18) (2001) 10037.

[17] C. L. Vizcarra, S. L. Mayo, Electrostatics in computational protein design, Current opinion in chemical biology 9 (6) (2005) 622–626.

[18] J. D. Jackson, R. F. Fox, Classical electrodynamics, American Journal of Physics 67 (1999) 841.

[19] W. Im, M. S. Lee, C. L. Brooks, Generalized born model with a simple smoothing function, Journal of computational chemistry 24 (14) (2003) 1691–1702.

[20] B. Jayaram, Y. Liu, D. Beveridge, A modification of the generalized born theory for improved estimates of solvation energies and pk shifts, The Journal of chemical physics 109 (1998) 1465.

[21] P. Politzer, J. M. Seminario, Modern density functional theory: a tool for chemistry: a tool for chemistry, Vol. 2, Elsevier, 1995.

[22] F. H. Stillinger, C. W. David, Polarization model for water and its ionic dissociation products, The Journal of Chemical Physics 69 (4) (1978) 1473–1484.

[23] A. A. Kornyshev, G. Sutmann, Nonlocal dielectric saturation in liquid water, Physical review letters 79 (18) (1997) 3435.

[24] D. W. Gruen, S. Marčelja, Spatially varying polarization in water. a model for the electric double layer and the hydration force, Journal of the Chemical Society, Faraday Transactions 2: Molecular and Chemical Physics 79 (2) (1983) 225–242.

[25] J. E. Nielsen, G. Vriend, Optimizing the hydrogen-bond network in poisson–boltzmann equation-based pka calculations, Proteins: Structure, Function, and Bioinformatics 43 (4) (2001) 403–412.

[26] A. Kornyshev, A. Rubinshtein, M. Vorotyntsev, Model nonlocal electrostatics. i, Journal of Physics C: Solid State Physics 11 (1978) 3307.

[27] M. Vorotyntsev, Model nonlocal electrostatics. ii. spherical interface, Journal of Physics C: Solid State Physics 11 (1978) 3323.

[28] K. Sharp, B. Honig, Calculating total electrostatic energies with the nonlinear poisson-boltzmann equation, Journal of Physical Chemistry 94 (19) (1990) 7684–7692.

[29] M. Holst, The poisson-boltzmann equation: analysis and multilevel numerical solution, Ph.D. thesis, University of Illinois (1994).

[30] F. Fogolari, J. M. Briggs, On the variational approach to poisson-boltzmann free energies, Chemical Physics Letters 281 (1-3) (1997) 135–139.

[31] P. Koehl, Electrostatics calculations: latest methodological advances, Current opinion in structural biology 16 (2) (2006) 142–151.

[32] P. Grochowski, J. Trylska, Continuum molecular electrostatics, salt effects, and counterion bindinga review of the poisson–boltzmann theory and its modifications, Biopolymers 89 (2) (2008) 93–113.

[33] D. Xie, New solution decomposition and minimization schemes for poisson–boltzmann equation in calculation of biomolecular electrostatics, Journal of Computational Physics.

[34] P. Debye, E. Hückel, De la theorie des electrolytes. i. abaissement du point de congelation et phenomenes associes., Physikalische Zeitschrift 24 (9) (1923) 185–206.

[35] N. Baker, M. Holst, F. Wang, Adaptive multilevel finite element solution of the poisson–boltzmann equation ii. refinement at solvent-accessible surfaces in biomolecular systems, Journal of Computational Chemistry 21 (15) (2000) 1343–1352.

[36] M. Holst, N. Baker, F. Wang, Adaptive multilevel finite element solution of the poisson–boltzmann equation i. algorithms and examples, Journal of Computational Chemistry 21 (15) (2000) 1319–1342.

[37] B. Luty, M. Davis, J. McCammon, Solving the finite-difference non-linear poisson–boltzmann equation, Journal of computational chemistry 13 (9) (1992) 1114–1118.

[38] W. Geng, R. Krasny, A treecode-accelerated boundary integral poisson-boltzmann solver for electrostatics of solvated biomolecules, Journal of Computational Physics.

[39] B. Lu, Y. Zhou, M. Holst, J. McCammon, Recent progress in numerical methods for the poisson–boltzmann equation in biophysical applications, Communications in Computational Physics 3 (5) (2008) 973–1009.

[40] W. Rocchia, E. Alexov, B. Honig, Extending the applicability of the nonlinear poisson-boltzmann equation: Multiple dielectric constants and multivalent ions, The Journal of Physical Chemistry B 105 (28) (2001) 6507–6514.

[41] D. Xie, S. Zhou, A new minimization protocol for solving nonlinear poisson–boltzmann mortar finite element equation, BIT Numerical Mathematics 47 (4) (2007) 853–871.

[42] D. Xie, J. Li, A new analysis of electrostatic free energy minimization and poisson–boltzmann equation for protein in ionic solvent, Nonlinear Analysis: Real World Applications 21 (2015) 185–196.

[43] S. Unni, Y. Huang, R. M. Hanson, M. Tobias, S. Krishnan, W. W. Li, J. E. Nielsen, N. A. Baker, Web servers and services for electrostatics calculations with apbs and pdb2pqr, Journal of computational chemistry 32 (7) (2011) 1488–1491.

[44] S. Sarkar, S. Witham, J. Zhang, M. Zhenirovskyy, W. Rocchia, E. Alexov, Delphi web server: A comprehensive online suite for electrostatic calculations of biological macromolecules and their complexes, Communications in computational physics 13 (1) (2013) 269.

[45] N. Smith, S. Witham, S. Sarkar, J. Zhang, L. Li, C. Li, E. Alexov, Delphi web server v2: incorporating atomic-style geometrical figures into the computational protocol, Bioinformatics 28 (12) (2012) 1655–1657.

[46] S. Jo, M. Vargyas, J. Vasko-Szedlar, B. Roux, W. Im, Pbeq-solver for online visualization of electrostatic potential of biomolecules, Nucleic Acids Research 36 (suppl 2) (2008) W270–W275.

[47] R. Luo, L. David, M. K. Gilson, Accelerated poisson–boltzmann calculations for static and dynamic systems, Journal of computational chemistry 23 (13) (2002) 1244–1253.

[48] D. Chen, Z. Chen, C. Chen, W. Geng, G.-W. Wei, Mibpb: A software package for electrostatic analysis, Journal of computational chemistry 32 (4) (2011) 756–770.

[49] Y. Jiang, Y. Xie, J. Ying, D. Xie, Z. Yu, Sdpbs web server for calculation of electrostatics of ionic solvated biomolecules, Molecular Based Mathematical Biology 3 (1).

[50] M. Gouy, Sur la constitution de la charge electrique a la surface d'un electrolyte, J. Phys. Theor. Appl. 9 (1) (1910) 457–468.

[51] D. L. Chapman, Li. a contribution to the theory of electrocapillarity, The London, Edinburgh, and Dublin Philosophical Magazine and Journal of Science 25 (148) (1913) 475–481.

[52] M.-J. Hsieh, R. Luo, Physical scoring function based on amber force field and poisson–boltzmann implicit solvent for protein structure prediction, Proteins: Structure, Function, and Bioinformatics 56 (3) (2004) 475–486.

[53] T. Lazaridis, M. Karplus, Effective energy functions for protein structure prediction, Current opinion in structural biology 10 (2) (2000) 139–145.

[54] V. K. Misra, D. E. Draper, Mg 2+ binding to trna revisited: The nonlinear poisson-boltzmann model, Journal of molecular biology 299 (3) (2000) 813–825.

[55] D. Boda, W. R. Fawcett, D. Henderson, S. Sokołowski, Monte carlo, density functional theory, and poisson–boltzmann theory study of the structure of an electrolyte near an electrode, The Journal of chemical physics 116 (16) (2002) 7170–7176.

[56] D. Jiao, P. A. Golubkov, T. A. Darden, P. Ren, Calculation of protein–ligand binding free energy by using a polarizable potential, Proceedings of the National Academy of Sciences 105 (17) (2008) 6290–6295.

[57] J. Che, J. Dzubiella, B. Li, J. McCammons, Electrostatic free energy and its variations in implicit solvent models, J. Phys. Chem. B 112 (10) (2008) 3058–3069.

[58] V. Jadhao, F. J. Solis, M. O. de la Cruz, Free-energy functionals of the electrostatic potential for poisson-boltzmann theory, Physical Review E 88 (2) (2013) 022305.

[59] C. Bertonati, B. Honig, E. Alexov, Poisson-boltzmann calculations of nonspecific salt effects on protein-protein binding free energies, Biophysical journal 92 (6) (2007) 1891–1899.

[60] V. S. Bryantsev, M. S. Diallo, W. A. Goddard, p k a calculations of aliphatic amines, diamines, and aminoamides via density functional theory with a poisson-boltzmann continuum solvent model, The Journal of Physical Chemistry A 111 (20) (2007) 4422–4430.

[61] Y. H. Jang, W. A. Goddard, K. T. Noyes, L. C. Sowers, S. Hwang, D. S. Chung, p k a values of guanine in water: Density functional theory calculations combined with poisson-boltzmann continuum-solvation model, The Journal of Physical Chemistry B 107 (1) (2003) 344–357.

[62] E. Alexov, E. L. Mehler, N. Baker, A. M Baptista, Y. Huang, F. Milletti, J. Erik Nielsen, D. Farrell, T. Carstensen, M. H. Olsson, et al., Progress in the prediction of pka values in proteins, Proteins: Structure, Function, and Bioinformatics 79 (12) (2011) 3260–3275.

[63] P. Weetman, S. Goldman, C. Gray, Use of the poisson-boltzmann equation to estimate the electrostatic free energy barrier for dielectric models of biological ion channels, The Journal of Physical Chemistry B 101 (31) (1997) 6073–6078.

[64] G. Moy, B. Corry, S. Kuyucak, S.-H. Chung, Tests of continuum theories as models of ion channels. i. poisson- boltzmann theory versus brownian dynamics, Biophysical Journal 78 (5) (2000) 2349–2363.

[65] T. J. Marrone, J. M. Briggs, and, J. A. McCammon, Structure-based drug design: computational advances, Annual review of pharmacology and toxicology 37 (1) (1997) 71–90.

[66] T. P. Lybrand, Ligand—protein docking and rational drug design, Current opinion in structural biology 5 (2) (1995) 224–228.

[67] M. R. Reddy, M. D. Erion, Free energy calculations in rational drug design, Springer Science & Business Media, 2001.

[68] P. Bopp, A. Kornyshev, G. Sutmann, Static nonlocal dielectric function of liquid water, Physical review letters 76 (8) (1996) 1280–1283.

[69] A. Hildebrandt, R. Blossey, S. Rjasanow, O. Kohlbacher, H.-P. Lenhof, Novel formulation of nonlocal electrostatics, Physical review letters 93 (10) (2004) 108104.

[70] M. V. Basilevsky, G. N. Chuev, Nonlocal solvation theories, Continuum Solvation Models in Chemical Physics: From Theory to Applications (2008) 94.

[71] Z. Zhou, P. Payne, M. Vasquez, N. Kuhn, M. Levitt, Finite-difference solution of the poisson–boltzmann equation: Complete elimination of self-energy, Journal of computational chemistry 17 (11) (1996) 1344–1351.

[72] L. Chen, M. Holst, J. Xu, The finite element approximation of the nonlinear poisson-boltzmann equation, Siam J. Numer. Anal 45 (6) (2007) 2298–2320.

[73] B. Li, Minimization of electrostatic free energy and the poisson-boltzmann equation for molecular solvation with implicit solvent, SIAM J. Math. Anal 40 (6) (2009) 2536–2566.

[74] E. Mechtly, The International System of Units: Physical Constants and Conversion Factors, Vol. 7012, Scientific and Technical Information Division, National Aeronautics and Space Administration, 1964.

[75] S. C. Brenner, R. Scott, The mathematical theory of finite element methods, Vol. 15, Springer, 2008.

[76] D. Xie, H. W. Volkmer, A modified nonlocal continuum electrostatic model for protein in water and its analytical solutions for ionic born models, COMMUNICATIONS IN COMPUTATIONAL PHYSICS 13 (1) (2013) 174–194.

[77] A. Logg, G. Wells, Dolfin: Automated finite element computing, ACM Transactions on Mathematical Software (TOMS) 37 (2) (2010) 20.

[78] M. Alnæs, J. Blechta, J. Hake, A. Johansson, B. Kehlet, A. Logg, C. Richardson, J. Ring, M. E. Rognes, G. N. Wells, The fenics project version 1.5, Archive of Numerical Software 3 (100).

[79] Z. Yu, M. J. Holst, Y. Cheng, J. A. McCammon, Feature-preserving adaptive mesh generation for molecular shape modeling and simulation, Journal of Molecular Graphics and Modelling 26 (8) (2008) 1370–1380.

[80] H. Si, A. TetGen, A quality tetrahedral mesh generator and three-dimensional delaunay triangulator, Weierstrass Institute for Applied Analysis and Stochastic, Berlin, Germany.

[81] F. C. Bernstein, T. F. Koetzle, G. J. Williams, E. F. Meyer, M. D. Brice, J. R. Rodgers, O. Kennard, T. Shimanouchi, M. Tasumi, The protein data bank, European Journal of Biochemistry 80 (2) (1977) 319–324.

[82] H. M. Berman, T. Battistuz, T. Bhat, W. F. Bluhm, P. E. Bourne, K. Burkhardt, Z. Feng, G. L. Gilliland, L. Iype, S. Jain, et al., The protein data bank, Acta Crystallographica Section D: Biological Crystallography 58 (6) (2002) 899–907.

[83] D. M. Beazley, et al., Swig: An easy to use tool for integrating scripting languages with c and c++.

[84] P. Peterson, F2py: a tool for connecting fortran and python programs, International Journal of Computational Science and Engineering 4 (4) (2009) 296–305.

[85] D. Xie, Y. Jiang, L. R. Scott, Efficient algorithms for a nonlocal dielectric model for protein in ionic solvent, SIAM Journal on Scientific Computing 35 (6) (2013) B1267–B1284.

[86] J. Ahrens, B. Geveci, C. Law, Paraview: An end-user tool for large-data visualization, The Visualization Handbook (2005) 717.

CURRICULUM VITAE

Yi Jiang

Place of birth: Hunan, China

Education

Ph.D in Mathematics, University of Wisconsin-Milwaukee, US, 2016

M.S. in Mathematics, Hunan University, China, 2010

B.S. in Information and Computational Sciences, Hunan University, China, 2007

Employment

- Teaching Assistant and Research Assistant, Department of Mathematical Sciences, University of Wisconsin-Milwaukee, US, 2010-2016

- Teaching Assistant, College of Mathematics and Econometrics, Hunan University, China, 2008-2010

Awards

1. Research Excellence Award, UW-Milwaukee, May 2015

2. Morris and Miriam Marden Award, UW-Milwaukee, May 2015

3. Mark Lawrence Teply Award, UW-Milwaukee, May 2014

4. Chancellor's Graduate Student Award, UW-Milwaukee, 2013 – 2016

Publications

1. D. Xie, Y. Jiang, A Nonlocal Modified Poisson?Boltzmann Equation and Finite Element Solver for computing Electrostatics of Biomolecules, Journal of Computational Physics (2016), http://dx.doi.org/10.1016/j.jcp.2016.06.028.

2. Y. Jiang, Y. Xie, J. Ying, D. Xie, and Z. Yu: SDPBS web server for calculation of electrostatics of ionic solvated biomolecules, Molecular Based Mathematical Biology, Vol. 3, pages 179-196, 2015.

3. L. R. Scott, Y. Jiang, and D. Xie: Comparison of a nonlocal dielectric model with a discontinuous model, University of Chicago Technical Report TR-2015-06, 2015.

4. Y. Jiang, J. Ying, and D. Xie: A Poisson-Boltzmann Equation Test Model for Protein in Spherical Solute Region and its Applications, Molecular Based Mathematical Biology, Vol. 2, pages 86-97, 2014.

5. D. Xie, Y. Jiang, and L. R. Scott: Efficient algorithms for solving a nonlocal dielectric model for protein in ionic solvent, Vol. 35, No. 6, pages B1267-1284, SIAM Journal on Scientific Computing, 2013.

6. D. Xie, Y. Jiang, P. Brune, and L. R. Scott: A fast solver for a nonlocal dielectric continuum model, SIAM Journal on Scientific Computing, Vol. 34, No. 2, B107-B126, 2012.